Noname manuscript No.
(will be inserted by the editor)

Energetic Charged Particles Above Thunderclouds

Martin Füllekrug[1], Declan Diver[2], Jean-Louis Pinçon[3], Alan D.R. Phelps[4], Anne Bourdon[5], Christiane Helling[6], Elisabeth Blanc[7], Farideh Honary[8], Giles Harrison[9], Jean-André Sauvaud[10], Jean-Baptiste Renard[3], Mark Lester[11], Michael Rycroft[12], Mike Kosch[8,13], Richard B. Horne[14], Serge Soula[15], and Stéphane Gaffet[16]

Received: date / Accepted: date

[1] Martin Füllekrug
University of Bath
Dept. of Electronic and Electrical Engineering
Bath, BA2 7AY, UK

[2] Declan Diver
University of Glasgow
School of Physics and Astronomy, Kelvin Building
Glasgow, G12 8QQ, UK

[3] Jean-Louis Pinçon and Jean-Baptiste Renard
Laboratoire de Physique et Chimie de l'Environnement et de l'Espace
3A avenue de la Recherche Scientifique, 45071 Orléans Cedex 2, France

[4] Alan D.R. Phelps
University of Strathclyde
Dept. of Physics, John Anderson Building
107 Rottenrow, Glasgow, G4 0NG, UK

[5] Anne Bourdon
Laboratoire d'Energétique Moléculaire et Macroscopique, Combustion,
CNRS, UPR 288,
Grande voie des vignes, 92295 Châtenay-Malabry, France

[6] Christiane Helling
University of St Andrews
School of Physics and Astronomy
North Haugh, St Andrews, KY16 9SS, UK

[7] Elisabeth Blanc
Commissariat à l'Energie Atomique
Laboratoire de Géophysique, 91680 Bruyères le Châtel, France

[8] Farideh Honary and Mike Kosch
Lancaster University
Physics Department
Lancaster, LA1 4YB, UK

[9] Giles Harrison

Abstract The French government has committed to launch the satellite TARANIS to study transient coupling processes between the Earth's atmosphere and near-Earth space. The prime objective of TARANIS is to detect energetic charged particles and hard radiation emanating from thunderclouds. The British Nobel prize winner C.T.R. Wilson predicted lightning discharges from the top of thunderclouds into space almost a century ago. However, new experiments have only recently confirmed energetic discharge processes which transfer energy from the top of thunderclouds into the upper atmosphere and near-Earth space; they are now denoted as transient luminous events, terrestrial gamma ray flashes and relativistic electron beams. This meeting report builds on the current state of scientific knowledge on the physics of plasmas in the laboratory and naturally occurring plasmas in the Earth's atmosphere to propose areas of future research. The report specifically reflects presentations delivered by the members of a novel Franco-British collaboration during a meeting at the French Embassy in London held in November 2011. The scientific subjects of the report tackle ionization processes leading to electrical discharge processes, observations of transient luminous events, electromagnetic emissions, energetic charged particles and their impact on the Earth's atmo-

University of Reading
Dept. of Meteorology
243 Earley Gate, Reading, RG6 6BB, UK

[10] Jean-André Sauvaud
Centre d'Etude Spatiale des Rayonnements/IRAP
9 Av du Colonoel Roche, 31028 Toulouse Cedex 4, France

[11] Mark Lester
University of Leicester
Dept. of Physics and Astronomy
University Road, Leicester LE1 7RH, UK

[12] Michael Rycroft
CAESAR Consultancy
35 Millington Road, Cambridge CB3 9HW, UK

[13] Mike Kosch also at
University of KwaZulu-Natal
School of Physics
Durban 4000
South Africa

[14] Richard B. Horne
British Antarctic Survey
Madingley Road, Cambridge, CB3 0ET, UK

[15] Serge Soula
Observatoire Midi-Pyrénées
Laboratoire d'Aérologie
14 Avenue Edouard Belin, 31400 Toulouse, France

[16] Stéphane Gaffet
Laboratoire Souterrain à Bas Bruit (LSBB)
La Grande Combe, 84400 Rustrel, France

sphere. The importance of future research in this area for science and society, and towards spacecraft protection, is emphasized.

Keywords Relativistic Atmospheric Electrodynamics

Contents

1 Introduction

The French government has committed ∼50 million Euro and ∼200 man-years to launch the microsatellite TARANIS of the Centre National d'Etudes Spatiales (CNES). The objective of TARANIS is to study transient energy transfer processes between the Earth's atmosphere and near-Earth space, with an emphasis on the detection of energetic charged particles and hard radiation emanating from thunderclouds (Lefeuvre et al., 2008; Blanc et al., 2007). Electrical discharge processes coupling the tops of thunderclouds with space were first predicted almost a century ago. However, new experiments have only recently discovered energetic discharge processes which are now denoted as transient luminous events, especially sprites (Pasko, 2010; Neubert et al., 2008; Füllekrug et al., 2006; Rakov and Uman, 2003; Sentman et al., 1995; Franz et al., 1990), terrestrial gamma ray flashes (Tavani et al., 2011; Smith et al., 2005; Fishman et al., 1994) and relativistic electron beams (Carlson et al., 2011; Füllekrug et al., 2011b; Briggs et al., 2011; Füllekrug et al., 2011a; Cohen et al., 2010;

Füllekrug et al., 2010; Carlson et al., 2009; Dwyer et al., 2008) (Figure 1).

A consolidation of the corresponding plasma physics in the laboratory and in the natural environment of the Earth's atmosphere enables the development of novel observational techniques to maximize the science return from the French satellite TARANIS. This topic of research is currently experiencing an exponential increase of citations which is predicted to accelerate as the planned space missions approach their launch date; this is so because plasma physics journals exhibit very high impact factors (Figure 2).

This report provides a description of the background and context (chapter 2) of the subsequent four different science themes which build on each other in a logical sequence. The first theme is concerned with the ionization processes of a neutral gas towards the formation of plasmas and subsequent discharges processes (chapter 3). The second theme addresses observations of transient luminous events above thunderclouds and their effects on the Earth's atmosphere (chapter 4). The third theme is associated with electromagnetic emissions of lightning discharges and energetic charged particle beams (chapter 5). The fourth theme is specifically concerned with energetic charged particles and their impact on the Earth's atmosphere and near Earth-space (chapter 6). These four themes are discussed in detail in the corresponding sections 3.1-3.6, 4.1-4.4, 5.1-5.4 and 6.1-6.4. Each section reflects the contribution of an attendant of the meeting at the French Embassy and tends to cover previous research, ongoing work and possible future directions. Given the breadth of the field, the given references are intended to support the specific individual contributions and they are therefore limited to fit the restricted length of this meeting report.

Transient events which couple the Earth's atmosphere to near-Earth space through hard radiation are named terrestrial gamma ray flashes (Tavani et al., 2011; Smith et al., 2005; Fishman et al., 1994). Current knowledge suggests that they are caused by upward propagating leader discharges inside thunderclouds (Lu et al., 2011; Shao et al., 2010; Stanley et al., 2006, and references therein) and are a natural consequence of intracloud discharges (Xu et al., 2012; Celestin and Pasko, 2012; Østgaard et al., 2012, and references therein) or possibly relativistic feedback discharges inside thunderclouds (Dwyer, 2012). The rapidly growing volume of literature in this research arena is reviewed by Dwyer et al. (2012) and it is therefore not considered here in detail.

2 Background and context

Upward electrical discharge processes coupling the top of a thunderstorm to the ionosphere were first predicted theoretically by the Nobel prize winner C.T.R. Wilson (Wilson, 1924, 1921, 1916). His electric field observations on the ground led him to picture a thunderstorm as an electrical dipole, having a

positive charge at the top and a negative charge at the bottom, with a potential difference of ∼1000 MV between them. This result led on to him believing that the ionosphere was at a potential approaching +1MV with respect to the Earth's surface (MacGorman and Rust, 1998, chapter 3). It is now realised that both of these values are overestimates; the potential difference between the top and bottom of a thundercloud is unlikely to exceed 150 MV, and the ionospheric potential is typically +250 kV. It is also realised now that there is often a region of positive charge below the negatively charged region (MacGorman and Rust, 1998, chapter 3).

Rycroft et al. (2012, 2008) and Rycroft and Harrison (2011) describe the modus operandi of the global circuit which was first conceived by Wilson (1929, 1921). Thunderstorms are one of the major generators in the circuit, and the other is due to electrified rain and shower clouds. Together, above disturbed weather regions, these drive a total global current of ∼1-2 kA up to the ionosphere. Ionization is created at all heights in the atmosphere by galactic cosmic rays and, just above the land surface, by the radioactive gas radon emanating from the surface. The ionosphere is an excellent conductor; it is essentially an equipotential surface at ∼+250 kV with respect to the Earth's surface. A total global current of ∼1-2 kA flows down to the Earth's surface through the fair and semi-fair weather regions of the atmosphere which are remote from thunderstorms. The height profile of the electrical conductivity of the atmosphere is the most crucial parameter of the global electric circuit (Rycroft et al., 2007; Rycroft and Odzimek, 2010). The circuit is completed through the good conducting land and ocean surfaces, and via point discharge currents up to the bottoms of thunderstorms.

Critical areas of global circuit research relating to thunderstorms for the future are: (a) the need for experimental studies to find out how much of the current flowing in the global circuit is produced by thunderstorms and how much is produced by electrified rain/shower clouds (Wilson, 1929), (b) the investigation of the influence of cosmic rays and magnetospheric phenomena on thunderstorm global circuit generators and also on the return part of the circuit, (c) the signatures of external influences such as associated with Forbush decreases of cosmic ray fluxes, or other space weather effects, and (d) the necessity for novel experiments carried out in space, either as independent missions such as TARANIS or aboard the International Space Station.

3 Ionization of plasmas and electrical discharge processes

The ionization of neutral gas and the propagation of ionization fronts (3.1) leads to small scale streamer discharges in laboratory experiments (3.2). In the Earth's atmosphere, dust and aerosols could potentially assist the formation of energetic charged particles (3.3). This speculative mechanism may be associated with electrified sporadic aerosol layers in the stratosphere (3.4)

which, along with grain-grain interactions, may result in the electrical charging of dust (3.5) which can lead to subsequent small scale streamer discharges in complex dusty plasmas (3.6).

3.1 Propagation of ionization fronts

This section describes the foundations of laboratory plasma discharges (compare with section 3.2) and the behavior of energetic electrons under the influence of a magnetic field which is relevant in the Earth's upper atmosphere (compare with section 6.1 and 6.2) and near-Earth space (compare with section 6.3 and 6.4).

The ionization of a neutral gas has a long history of scientific investigation, originating from Townsend's seminal 1901 paper (Townsend, 1901), in which the ionization coefficients were first described. Electron avalanches are a fundamental step in the breakdown process, and the subsequent formation of conducting channels that permit the rapid transition to full ionization (in the case of laboratory plasmas) or transient energetic electrical phenomena (such as lightning). The experimental investigation of sub-nanosecond evolution of the avalanches into streamers is a challenging procedure, due to the very tiny length and time scales involved (Nijdam et al., 2010). Even for the relativistic electron avalanches in air (for example, Babich et al., 2004) the relaxation timescales are still in tens of ns, even though the scale-lengths are in metres. There has been significant progress in numerical simulations of the early stages of avalanche and streamer formation, both fully particle in cell (Dowds et al., 2003; MacLachlan et al., 2009) and in hybrid codes (Li et al., 2012). Each approach has its own merits, in that the former is able to recover fully the charged-particle distribution functions, and the latter is particularly efficient in keeping the computational overhead to reasonable proportions.

These numerical insights allow a greater understanding of the collective non-linear behaviour of electrons in such non-equilibrium situations, particularly with regard to the population of energetic electrons in the Earth's upper atmosphere. In the magnetically constrained calculations of MacLachlan et al. (2009), an initial spherical cloud of electrons expands under self-repulsion into an elongated structure with the long axis aligned with the magnetic field, at the tips of which are the most energetic electrons (see Figure 3). The reason for this is clear: the inhibition of perpendicular transport by the strong magnetic field means that the parallel-directed electrons experience the electrostatic repulsion from the other electrons for longer than had there been no magnetic field at all. Hence, any mechanism that delays the dispersion of free charge in an anisotropic way can provide a means by which energetic particle fluxes can be produced along a particular direction, draining energy from the inhibited population in the anisotropic evolution.

3.2 Laboratory streamer discharges

This section describes in more detail laboratory streamer discharges (compare with section 3.1) and the application of these concepts to sprites in the middle atmosphere (compare with section 4.1).

In recent years, plasma discharges at atmospheric pressure have gained popularity due to their potential for a wide range of applications including plasma-assisted combustion, biomedical treatment, decontamination and thin film coatings (Van Veldhuizen, 2000; Fridman et al., 2005). These discharges are particularly interesting for applications as they efficiently produce active species in well-controlled environments. Furthermore, the use of atmospheric pressure versus vacuum technologies reduces costs. In plasma processing reactors, discharges are generally produced in small gas gaps (typically of a few millimetres) and interact with gas flows.

At atmospheric pressure, plasma discharges usually operate in a filamentary mode, characterized by the initial propagation in the gas gap of an ionization front, also called streamer, with a high electron number density (typically greater than $10^{14}/\mathrm{cm}^3$) in a narrow filament (typical radius of 100 μm). This discharge mode produces high concentrations of active species and can effectively enhance the reactivity to a level sufficient for many applications of interest such as plasma-assisted flame ignition. Yet, filamentary discharges induce a significant degree of gas heating, which may be undesirable for certain applications that are adversely affected by heat. One example is the treatment of sensitive surfaces or electronic equipment. Furthermore, the localization of the discharge is also undesirable for applications like thin-film coating and the treatment of large surfaces.

Therefore, many studies in recent years have been devoted to obtain diffuse discharges at atmospheric pressure with nanosecond repetitively pulsed discharges (NRPD) between pin-pin electrodes (Pai et al., 2010) or dielectric barrier discharges with resistive-backing (Massines et al., 1998). Diffuse discharges are characterized by a relatively low electron concentration and a larger excitation volume than those produced by typical filamentary discharges, with a negligible level of gas heating. These diffuse discharges thus are an interesting alternative to filamentary discharges and open a complementary range of applications.

In large-scale discharges at high altitudes, as in sprites (see for example Siingh et al., 2012, for a recent review of tranient luminous events), it is interesting to note that the observed fine structures are similar to small-scale streamers and are only scaled by the reduced air density at high altitudes (Pasko, 2007; Ebert et al., 2010). However, due to the change of densities, the relative importance of some processes (such as photoionization source terms) are enhanced at high altitudes in comparison to ground level. Then, the prob-

ability of discharge branching due to a low preionization ahead of the streamer increases as altitude decreases (Liu and Pasko, 2004; Nijdam et al., 2010). It is also interesting to note that for the air densities corresponding to 0-70 km altitudes, the strong reduction of electron loss rates with the reduction of air pressure leads to a significant acceleration of the gas heating as altitude increases (Riousset et al., 2010). At ground level and at high altitudes, the peak electric field in the discharge front may be derived from recorded optical emissions of the discharge, and a detailed study is presented by Bonaventura et al. (2011). Finally, a few studies have been carried out on the production of energetic electrons by high altitude streamers (Chanrion and Neubert, 2010) and their implication in terrestrial gamma ray flashes (Celestin and Pasko, 2010). For applications at ground level, this subject has started to be studied recently as the applied voltages of the latest pulse generators increase and the voltage rise times decrease, which may favour the production of energetic electrons (Nguyen et al., 2010). The challenge now is to simulate the time-space multi-scale character of the coupling of the discharge physics with chemistry, diffusion, gas heating and convection.

3.3 Influence of dust and aerosols on streamer formation

This section considers an established mechanism to create energetic charged particles in pulsed laboratory systems. It is speculated that this mechanism may also lead to the formation of energetic charged particles in the stratosphere. The proposed mechanism may be assisted by the presence of electrified sporadic aerosol layers (compare with section 3.4), grain-grain interactions (compare with section 3.5) and streamer discharges in dusty plasmas (compare with section 3.6). Whether the associated microscopic small-scale electric fields help to setup the large scale electric fields which are required for the formation of elongated energetic charged particle beams in the Earth's atmosphere remains to be investigated in future studies.

Dust or aerosols above thunderclouds could potentially play a very significant role in the creation of energetic charged particles. The scenario envisaged is as follows (see Figure 4): a large thundercloud has excess negative charge just above its upper side, and positive just below its lower surface. Free electrons are produced at the cloud top in response to the influx of electrons resulting from the lightning strike at the cloud underside; until this point, the cloud is electrically neutral albeit charge-separated. However, gaining an excess of electrons allows a repulsive electric field to develop which launches free electrons off the topside of the cloud. The spectrum of energies of such electrons really depends on the initial/evolving geometry and the parameter regime (e.g. for restricted electron transport as described in MacLachlan et al. (2009)), but we envisage that some will reach ionizing energies and produce a positive ion population. A fraction of the free electrons will attach to the macroscopic particles that constitute the aerosol or dust population above the

thundercloud, leaving a positive ion trail behind such that an electrostatic charged structure is created. The positive ions act as a seed potential to form an electric field with a radial component. Should there be another electron acceleration event from the top of the thundercloud in a shorter time interval than the positive ion transit time for quenching the dust charge, then these new electrons will be accelerated upwards in the electric field produced by the positive ion channel and the negatively charged dust grains or aerosols - acting as a guiding, accelerating field, and enhancing the initial impulse that caused them to be dislodged from the cloud top in the first place. The grains (aerosols) plus the positive ion trail will act as a lens, adding an electrostatic potential derived from the previous event that will enhance acceleration and constrain the lateral dispersion of the electrons, so contributing to the production of more energetic and beamed electrons. Such a harnessing of the previous charging cycle is common in pulsed laboratory systems. The closest laboratory concept is that of the hollow-cathode discharge, in which a strongly beamed electron distribution is produced from a cathode shaped in a partially-closed cylindrical configuration with an anode trigger just outside (e.g., Becker et al., 2006; Slevin and Harrison, 1975). In the thundercloud context, the analogy of the hollow cathode is the negatively-charged dust/aerosol structure above the cloud, and the anode is the positive ion trail from the previous discharge event. The challenge now is to simulate such an environment, building upon successful numerical work in sub-nanosecond avalanche studies combined with electrostatic enhancement from dust-charging processes.

3.4 Observations of electrified sporadic aerosol layers in the stratosphere

This section describes the presence of sporadic aerosol layers in the stratosphere which may be assisted by the charging of dust (compare with section 3.5) and result in the formation of energetic charged particles (compare with section 3.3).

Recent work has shown that the stratospheric background aerosol content is more complex than was expected (Renard et al., 2008, 2010). In the lower stratosphere, typically between 10 and 25 km altitude, the main population is composed of liquid aerosols coming from volcanic eruptions, although some solid particulates are present. It must be noticed that even moderate volcanic eruptions can inject aerosols into the middle atmosphere (Vernier et al., 2009). Above 25 km, some liquid aerosols can be found, but the main population seems to be solid particulates. Analyses of the GOMOS-Envisat satellite data has indicated that these particles are mainly soot, probably coming from biomass burning and from anthropogenic activities in the troposphere. These aerosols are then transported into the stratosphere, perhaps assisted by processes linked to the atmospheric electric field. Also particulates coming from meteoritic disintegration, and grains and soot coming from recondensation,

can be found in the middle and upper stratosphere.

Balloon-flights of the improved version of the STAC aerosol counter (Renard et al., 2008) have been performed, allowing the concentration and the size distribution of the submicronic liquid aerosols to be determined. STAC has allowed the presence of solid aerosols having diameters greater than $\sim$1 μm to be detected. For most of the flights, strong local enhancements of aerosol concentration were detected in the middle stratosphere, having a vertical extent on the order of $\sim$1 km, and a horizontal extent of less than a few tens of km.

During the last STAC flight, on 12 March 2011 from Kiruna (Northen Sweden), measurements of the charged aerosols were performed in the 5-25 km altitude range. On the same gondola, one STAC instrument was mounted with a deflecting system that prevents the charged aerosols from going inside the counting system, and another STAC was mounted without it. The measurements were conducted simultaneously during the balloon ascent and descent. Near the tropopause, at an altitude around $\sim$10 km, no significant charged aerosol content was detected within a total aerosol content variability of $\sim$30-50 %. On the contrary, in the middle troposphere and in the middle stratosphere, $\sim$80-90 % of the solid aerosols were electrically charged.

The STAC measurements have confirmed that the stratospheric solid aerosols can be charged and the vertical transport of such particulates could be related to the atmospheric electric field. The enhancement of the charged aerosol content in the middle stratosphere compared to the tropopause may be linked to spatial variations of the electric field. Finally, such solid aerosols could play a role in the formation of transient luminous events.

All these results and hypotheses need confirmation and new measurements. The polarity of the charged particulates was not measured by STAC, but a new version of the instrument will allow that to be determined. It is expected that balloon flights will be performed in 2013 with this new aerosol counter, coupled with atmospheric electric field measurements obtained using the gondolas of the LATMOS-CNRS team.

3.5 Electrified dust in the troposphere

This section discusses charging of dust in the troposphere. Similar mechanisms may be relevant for the electrification of sporadic aerosol layers in the stratosphere (compare with section 3.4) and may assist the formation of the energetic charged particles associated with streamer formation (compare with section 3.3).

Dust plays an important role in the radiative budget of the Earth's atmosphere, and hence the effect of charge on its behaviour may also be of relevance

to the climate system. Charging of dust can occur during its generation, or through the attachment of atmospheric molecular cluster ions formed by natural radioactivity or cosmic rays. The physical consequences of charging include the enhanced removal of charged particles by water droplets compared with the removal of neutral particles (Tripathi et al., 2006), and effects on coagulation behaviour. Alignment of charged aggregates in atmospheric electric fields is also possible, by analogy with that observed for ice in thunderstorm electric fields (Saunders and Rimmer, 1999). Vertical dust alignment has been inferred from polarimeter measurements, decreasing the optical thickness of the dust layer by the "Venetian blind effect" (Ulanowski et al., 2007). Whether this is electrical in origin is yet to be established, but, as the alignment influences the radiative properties of a dust layer, in situ measurements of charge in dust clouds are clearly needed to advance understanding.

Recent tropospheric measurements of dust charging used two different sensors carried on standard the weather balloons. The first sensor is an aerosol particle counter which measures particle size and number concentration using light scattered from particles drawn into a sampling chamber by an air pump. The second sensor is a dust charge sensor which consists of a 12 mm diameter spherical metal electrode, connected to an electrometer voltmeter. The impact from electrified particles on the electrode transfers charge which changes the electrode voltage. Dust charging has been been reported for Saharan dust, and volcanic plumes which are known readily to electrify (Mather and Harrison, 2006). Saharan dust measured over the Cape Verde Islands shows electrification in regions coincident with abundant particle concentrations (Figure 5 (a) and (b)) (Nicoll et al., 2011), and volcanic ash from the Icelandic volcano, Eyjafjallajökull, showed slight electrification at considerable distances from its source (Figure 5 (c) and (d)) (Harrison et al., 2010).

The experimental challenge of making such measurements is demanding, as the instrumentation may have to be deployed at short notice in harsh environments, but constraining the charge on dust and ash is essential to models which evaluate the physical importance of dust charging in the Earth's climate system.

3.6 Electrification of dusty extrasolar environments

This section describes the need for efficient discharge mechanisms in dusty plasmas in extraterrestrial planetary environments. It discusses the formation of self-propagating ionisation fronts starting with an electron avalanche (streamer) discharges in mineral clouds as a potential mechanism, which are the precursor for relatively large-scale discharge events (compare with section 3.3).

Transient luminous events are potentially powerful diagnostic tools also outside our solar system, due to their impact on the local environment and possibly due to a release of accelerated electrons into space. Studies have therefore been started to investigate charge processes in mineral clouds in planetary atmospheres, based on a model of kinetic dust formation (Helling and Woitke, 2006). An estimate illustrates the charges needed to exert an effect on the atmosphere environment. Local temperatures are so low that thermal ionisation is negligible, hence the charge balance in a dust-gas mixture without external sources of ionisation is driven by collisional processes with dust grains $dn_{\rm e}/dt = I_{\rm dust} - R_{\rm dust} = 0$:

$$N n_{\rm d}^2 \pi a^2 v_{\rm rel} - n_{\rm e} n_{\rm d} \pi a^2 c_{\rm e} = 0 \;\Rightarrow \frac{I_{\rm dust}}{R_{\rm dust}} \sim N \frac{n_{\rm d}}{n_{\rm e}} \frac{v_{\rm rel}}{c_{\rm e}}, \qquad (1)$$

with $n_{\rm e}$ and $n_{\rm d}$ the electron and the dust number density, respectively, N the number of charges produced by a collision, a the dust grain radius, $v_{\rm rel}$ a relative velocity, and $c_{\rm e}$ the electron thermal velocity. $I_{\rm dust}$ and $R_{\rm dust}$ are the constructive and destructive rates for electron production by dust collisions. An order of magnitude estimate for these parameters is for example given by, $\rm p_{gas} \sim 10^{-5}$ bar, $\rm T_{gas} \sim 1000$ K, $\rm n_d \sim 10^{-10}$ cm^{-3} (Helling et al., 2008a), $\rm v_{rel}^{drift} \sim 10^4$ cm s^{-1} (Witte et al., 2009), $\rm n_e \sim 0.076$ cm^{-3} for $\rm p_e \sim 10^{-14}$ dyn cm^{-2}, $\rm c_e = \sqrt{(2kT/m_e)} = 1.7 \times 10^7$ cms^{-1}.

Since the number density of dust grains is so much less than that of thermal electrons in planetary atmospheres, we require that the number of charges N produced by collisions must increase dramatically. We estimate that $I_{\rm dust}/R_{\rm dust} \sim 7 \cdot 10^{-13} N$, hence we require $N > 1.4 \cdot 10^{12}$ in the low-pressure part at $p_{\rm gas} \sim 10^{-5}$ bar of the cloud. Conditions are more favourable at higher pressures as fewer free charges would be needed. These numbers are, however, sufficiently large that it is unlikely that a simple collisional process alone will produce such high numbers (Helling et al., 2011b). Numerical simulations of streamer evolution suggest comparable numbers of $10^{13} - 10^{14}$ cm^2; three free charges form during the consecutive avalanches in the streamer (Dowds et al., 2003; **?**). Our results suggest that extraterrestrial atmosphere may not be in steady state, a fact that is known for the Earth atmosphere which undergoes non-equilibrium discharge events that participate in feeding the global atmospheric electric circuit.

We have shown that mineral dust clouds should be charged (Helling et al., 2011a) based on the results from a dust cloud formation model that described seed formation, surface growth and evaporation, sedimentation and element conservation in an oxygen-rich, hydrogen-dominated atmosphere environment (Woitke and Helling, 2003; Helling and Woitke, 2006; Helling et al., 2008b). These clouds are made of grains composed of minerals that are a mixture of oxides, silicates and iron (left of Figure 6). The volume contribution of each condensate changes with height in the atmosphere reflecting the height-dependent temperature inside the atmosphere. In addition, the grain sizes are

not constant, but grain sizes change with height and a whole distribution of grain radii, a, exists in each atmosphere layer as the efficiency of the dust formation processes changes (right of Figure 6). These cloud particles of different sizes frictionally couple to the turbulent atmospheric gas which greatly improves tribo-electric charging due to increased relative velocities.

A cloud particle of a size of 0.5 μm carrying a charge of $10^3 e$ (e.g, Desch and Cuzzi, 2000) has an electric field of $\sim 10^7$ V/m near its surface. If such two dust grains pass each other, a mini-capacitor exposing curved capacitor plates develops and a streamer event is initiated, (e.g., Dowds et al., 2003). Non-spherical effects will further affect the kinetic growth and the state of charge of an electrostaticaly charged cloud particle (Stark et al., 2007). Further it has been demonstrated that the streamer life time can be expected to be longer than the Coulomb recombination time, and that in certain parts of a mineral cloud several successive streamers can develop until the grains are neutralised by Coulomb recombination.

Transient luminous events should be expected to develop also from extrasolar (mineral) clouds as the superposition of streamer events is larger at the cloud top. Here, at a pressure level of $\leq\sim 10^{-6}$ bar, the electric breakdown field is 10^5 to 10^9 times lower than the $\sim$1 bar-values given for the solar system planets. It is interesting to notice that the chemical composition of extrasolar planets does not necessarily resemble the known examples in our solar system providing a test bed for our knowledge primarily developed on Earth.

4 Observations of transient luminous events

Transient luminous events can be observed optically with video cameras from the ground (4.1) and they may cause optical emissions in the F-region ionosphere (4.2). Sprites also produce infrasound chirps which are observed with acoustic networks (4.3). Optical emissions (4.4) of lightning discharges and transient luminous events are observed from space with satellites.

4.1 Optical observations of transient luminous events

This section describes thunderstorm activity in southern France and optical observations of transient luminous events which can also be observed from space (compare with section 4.4) and are similar to small scale streamer discharges in the laboratory (compare with section 3.2). Some transient luminous events are associated with infrasound signals (compare with section 4.3) and may be associated with faint illuminations of the F-region ionosphere (compare with section 4.2).

Transient Luminous Events are known since their first optical observation in the late 80s (Franz et al., 1990). This first event was later named “sprite”

when new cases were observed during dedicated campaigns a few years later (Sentman and Wescott, 1993; Boccippio et al., 1995). By analyzing recordings from cameras installed on board the Space Shuttle, Boeck et al. (1992) identified another kind of TLE as a transient airglow subsequently called "Emissions of Light and Very low frequency perturbations from Electromagnetic pulse Sources" (elves) to describe their physical origin (Fukunishi et al., 1996). Amorphous glows which are different from elves and which may precede sprites have been observed and are now named halos (e.g., Barrington-Leigh et al., 2001). Upward discharges rising from the cloud top were observed for the first time during an airborne campaign and are identified as blue jets (Wescott et al., 1995). Another upward discharge shooting up from the thundercloud and reaching altitudes within the lower ionosphere (70-90 km) was named gigantic jet (Pasko et al., 2002; Su et al., 2003).

Optical observations of transient luminous events (TLEs) are currently performed from several sites in southern France; these observations have been made for several years. The equipment at each site consists of a low-light charge-coupled device (CCD) camera (Watec 902H) mounted on a pan-tilt unit remotely controlled through the Internet. A 12 mm f/0.8 lens provides a 31^o field of view (FOV). The GPS time is inserted in the 20-ms resolution images by use of a video time inserter device. One of the stations is located at the Pic du Midi (42.93^o N, 0.14^o E, 2877 m altitude). TLE azimuth and elevation are deduced from the video imagery by using the software "Cartes du Ciel" (SkyCharts) by matching stars with those visible in the image. This method has an accuracy of less than $\sim$1 km at a distance of $\sim$300 km (Van der Velde et al., 2010). When a TLE is detected at several sites, each element of the TLE can be triangulated by use of the different observed azimuths.

Numerous sprites and other TLEs have been observed above storms throughout the year over land (France and Spain) or over the sea (the western Mediterranean Sea close to the Atlantic Ocean). Some TLEs and their parent storms have been analysed by assimilating various data sources (cloud top temperature from Meteosat satellite, cloud structure from radar reflectivity, lightning activity from several lightning detection networks, and ELF/VLF electromagnetic radiation from various radio receivers). Several characteristic aspects of the storm producing TLEs, different correlations between the type, shape, size and time delays of TLEs and characteristics of the associated lightning flashes have been reported (e.g., Neubert et al., 2008; Van der Velde et al., 2006; Soula et al., 2009, 2010). Figure 7 displays different types of TLEs observed at various distances (from 150 km to close to 900 km), locations and seasons throughout the year. These images correspond to 20-ms frames from the video imagery which include sprites, groups of sprites of different types (column, carrot, dancing sprite, jellyfish, ...), elves and halos (Barrington-Leigh et al., 2001). Figure 7 includes also an image of one of the five gigantic jets recorded with a camera at Réunion Island (Soula et al., 2011).

The shape of the sprite event in one frame can depend on its stage of development since it can last for several frames after the first streamer is triggered at an altitude of about 70 km. The number of sprite elements is very variable and can reach several tens in a group of columns. The elements in a group of sprites can be organized in a ring shape and may be horizontally displaced from the location of the parent lightning flash. Sometimes the sprite elements can be oriented towards the parent lightning flash (Neubert et al., 2008). The overwhelming majority of sprite-producing lightning flashes are positive cloud-to-ground (+CG) flashes occurring within the stratiform region of the storm (Van der Velde et al., 2006; Soula et al., 2009). The tendrils which develop downward below the luminous sprite body are much more numerous for carrot sprites. The diffuse light at the top of sprites is more developed for carrot sprites and can make the sprite look like a jellyfish. The carrot sprites can be associated with a halo which is generally produced earlier by the same flash which has a large peak current.

The typical frequency of sprite production for a storm during the favourable period is generally around 0.2 min^{-1}. However, several sprite events can be triggered by successive positive CG flashes within a very short time delay (typically <1 s) which indicates that the conditions are more favourable when a positive flash is rapidly produced after a previous flash (Soula et al., 2010). The elves are rather observed above storms over the sea and appear as luminous rings with a visible diameter of about 300 km. They can be either produced by positive or negative CG flashes with large peak currents. The gigantic jets have been observed to be preceded by intracloud lightning activity and carry negative charge out of the main cloud charge region (Soula et al., 2011). This confirms the theory proposed by (Krehbiel et al., 2008) based on a discharge triggered between unbalanced cloud charges to explain gigantic jets.

4.2 Optical observations of sprite-induced transient luminous events in the F-region ionosphere.

This section describes the possibility of faint illuminations of the F-region ionosphere associated with plasma resonances due to the electromagnetic pulse generated by intense lightning discharges, which are also known to cause the transient luminous events above thunderclouds in the middle atmosphere (compare with section 4.1).

It is now well known that pumping the F-region ionosphere with high-power high-frequency (HF, 2-10 MHz) radio waves may cause various plasma-instabilities and wave-particle interactions, which lead to electron acceleration up to several 10s of eV (e.g., Gustavsson et al., 2005), i.e. supra-thermal electron fluxes. Through collisions these high-energy electrons can produce all the optical emissions known in the natural aurora. The phenomenon is called the artificial aurora. Typical F-region optical emissions and their threshold ener-

gies are 630 nm (∼2 eV), 557.7 nm (∼4.2 eV), 777.4 nm (∼9 eV) and 844.6 nm (∼ 11 eV) from atomic oxygen as well as 427.8 nm (∼18.6 eV) from ionised molecular nitrogen. Figure 8 shows examples of artificial auroras generated by the high-power HF facility (Stubbe, 1996) at the European Incoherent SCATter radar facility (EISCAT), located in northern Norway (Rishbeth and van Eyken, 1993). See Kosch et al. (2007a) for a review of recent observations from several pump facilities around the world.

In addition to optical emissions, pumping the ionosphere with high-power HF radio waves produces a variety of other effects, including bulk electron temperature enhancements from a background of ∼1500 K up to ∼4000 K (e.g., Robinson et al., 1996), ion outflow (Kosch et al., 2010) as well as magnetic field-aligned meter-scale plasma irregularities called striations (e.g., Honary et al., 1999). All the above phenomena are associated with the upper-hybrid plasma resonance, which occurs in a magnetized plasma, and which is present a few km below the HF reflection altitude in the F-region ionosphere (e.g., Kosch et al., 2002). See Kosch et al. (2007b) for a discussion of relevant wave-particle interactions.

Plasma resonances leading to electron acceleration are found to be very sensitive to the aspect angle between the radio wave propagation direction and the Earth's magnetic field direction (e.g., Kosch et al., 2011); artificial auroras are likewise much more intense close to the magnetic zenith (Kosch et al., 2000). Unfortunately, only a small number of ionospheric pump facilities exist in the world and so it is not easy to quantify this effect properly. However, sprites and their parent lightning discharges are known to produce powerful radio waves over a broad spectrum (e.g., Füllekrug et al., 2011b; Singh et al., 2008; Farrell and Desch, 1992), including the HF band. This means that the upper-hybrid resonance can be stimulated for a wide altitude range in the F-region. Therefore, sprites make good, if intermittent, radio wave sources to study electron acceleration by wave-plasma resonance in the F-region at locations where pump facilities are not available. Since the sprite strike occurs mostly vertically, a doughnut of radiation, centred on the sprite similar to a vertical dipole radiator, is expected to propagate outwards in all directions except vertically. Hence, F-region wave-particle interactions are expected to occur several tens of km horizontally away from the sprite location. Our experience with ionospheric modification facilities is that k parallel to B enhances the production of optical emissions from accelerated electrons resulting from wave-plasma interactions. If sprite emissions are similar to a vertical dipole, then one would expect induced optical emissions to appear more readily at mid- and low latitudes rather than at high latitudes since a vertical dipole will have a radiation field of significant strength from the horizontal up to at least $\sim 45^o$ elevation angle. Optical emissions are excited with a radio wave flux above ~ 40 μW/m^2 in the F-layer ionosphere (Bryers et al., 2012, Fig. 5). To obtain the radio wave flux quantitatively requires knowledge of the source power as well as the D-layer ionosphere radio wave absorption, which can be

very significant at high frequencies. For controlled experiments where incoherent scatter radars are available, the power flux estimate can be done (Bryers et al., 2012). In principle, this can also be done for sprites, and could be a subject for future work. The resulting F-region optical emissions of known wavelengths can be detected from the ground as is commonly done for the auroras, both natural and artificial. From these calibrated multi-wavelength data, the energy spectrum of the accelerated electrons can be extracted (Gustavsson et al., 2005) for a wide range of aspect angles.

4.3 Infrasound from transient luminous events

This section describes the generation of infrasound signatures caused by transient luminous events above thunderclouds in the middle atmosphere (compare with section 4.1).

The possibility that transient luminous events (TLEs) radiate infrasound or acoustic waves in the atmosphere has been the subject of research for many years since the first TLE observations were made in the beginning of the 1990s. Such emissions can be the signature of specific processes occurring inside the TLE structure, such as the heating of ambient air. Such observations are difficult as these signals are observed several hundred seconds after the sprites. This delay corresponds to the propagation time at the sound velocity in the atmospheric waveguide formed between the ground and the temperature increases of the stratosphere and lower thermosphere. The first observations possibly related to sprites were performed in Sweden, in spite of the low thunderstorm activity in the high latitude regions compared with other regions of the Earth. Liszka (2004) observed chirp signals attributed to sprites while thunderstorms were located at distances of several hundred kilometers from the observation stations. Statistics have been obtained over 10 years and used to study some mechanisms (Liszka and Hobara, 2006).

The first infrasound signals unambiguously produced by sprites were observed in France. Chirp signals similar to those observed in Sweden were related one to one to sprites observed by cameras, using infrasound ray tracing models in a realistic atmosphere (Farges et al., 2005). The size of the sprite directly determines the infrasound signal duration of about several tens of seconds. This corresponds to the time difference between the propagation of infrasound coming from the nearest and farthest sides of the sprite. The chirp structure, or frequency dispersion, is the effect of the attenuation in the lower thermosphere where infrasound is reflected prior to detection on the ground. The first infrasound signal from the nearest side of the sprite is reflected at a higher altitude with a reduced high-frequency content, compared with the last signal generated from the farthest side reflected at a lower altitude with enhanced high-frequency content. Recent models of the weak air heating in streamer channels in sprites on the order of several degrees Kelvin explain the

production of the observed signals (Pasko and Snively, 2007).

The new infrasound stations composed of infrasound mini arrays measure elevation angle and azimuth from which infrasound propagation can be inferred when the propagation from a sprite to the station is direct at distances less than 100 km. Inversion localizes the infrasound origin inside the sprite structure at altitudes ranging from 40 to 90 km (Farges and Blanc, 2010). In this case inverted chirp signals are measured. This morphology of the infrasound signal reveals the general scaling of the diameters of the sprite streamers as being inversely proportional to the air density (De Larquier and Pasko, 2010). This methodology offers an opportunity for systematic sprite observations without the limitations on the field of view or nighttime imposed by camera observations. In this way, sprite occurrence rates can be determined by taking into account the detection efficiency (some sprites are not detected) and the false alarm rate (some events are not sprites) (Ignaccolo et al., 2006). It is therefore proposed to complement sprite infrasound observations with other observational technologies.

4.4 Observations of transient luminous events above thunderstorms from space

This section describes the observation of transient luminous events above thunderclouds from space (compare with section 4.1).

Up to now, TLEs have mainly been observed from space towards the horizon (Mende et al., 2006; Yair et al., 2004), where sprites and lightning are spatially distinguishable. TLE observations above thunderstorms are difficult because the sprites are superimposed on the intense emissions of the lightning below, and diffused by clouds. Such observations can be performed in the most intense emission line of sprites N2 1P at 762.7 nm which coincides with the molecular oxygen absorption band of the atmosphere. The optical emissions of lightning, produced at lower altitudes than sprites, are absorbed but they cannot be totally suppressed in this way. Two cameras, one in the main lightning emission band and the other in the sprite emission band have to be used to fully extract the sprite response by spectral differentiation (Blanc et al., 2006). Such a methodology has been validated on board the International Space Station by the experiment LSO (Lightning and Sprite Observations) (Blanc et al., 2004, 2006). This method will be used by the TARANIS satellite (Blanc et al., 2007; Lefeuvre et al., 2008) and by other space missions, such as GLIMS and ASIM. The interest of such observations from space at the nadir is the possibility to measure together TLEs and all hard radiations above thunderclouds which is needed for a better understanding of the processes involved.

5 Electromagnetic emissions from lightning discharges and electron beams

Electron beams can radiate electromagnetic waves which are observed in laboratory experiments (5.1). In the Earth's atmosphere, electromagnetic waves from lightning discharges can be observed with a spiral array of radio receivers (5.2). Upward beams of relativistic electrons emit radio waves from low frequencies of some tens to hundreds of kHz (5.3). Radio signatures of lightning discharges and transient luminous events are observed from space with satellites (5.4).

5.1 Electromagnetic radiation from electron beams

This section describes studies of electromagnetic radiation from electron beams in the laboratory which has been relevant for auroral emission processes (compare with section 6.1, 6.2 and 6.4) and may help to explain radio emissions from the middle atmosphere (compare with section 5.3).

Laboratory experiments in which relativistic electron beams with well-determined parameters are observed interacting with known gas mixtures, with and without applied magnetic fields, can provide a valuable complement to satellite and ground-based observations of naturally occurring phenomena. The observable emissions in these laboratory simulations include emitted spectra of ultraviolet, visible, infrared and longer wavelength (radio frequency, RF) electromagnetic radiation. As well as measuring the emitted spectral parameters, in situ measurements in the laboratory of the energetic particle beam velocity distributions, both before and after the interactions, can be recorded. These data are valuable in establishing self-consistent models of the energy transfer mechanisms involved (a) in accelerating the beams and (b) subsequently dissipating the energy of the beams via a number of processes including particle collisions and electromagnetic radiation production over several spectral ranges.

It has been understood for a long time that energetic electron beams passing through media, both with and without applied magnetic fields, can produce observable radiation by numerous mechanisms including bound-bound, free-bound and free-free atomic and molecular transitions, and that electron beams passing through an ionized medium can stimulate several types of collective instabilities (Allen and Phelps, 1977) that typically result in the emission of longer wavelength radiation. In the latter case depending upon the specific parameters of the interaction region the emitted electromagnetic radiation can be at the plasma frequency, the cyclotron frequency (Trakhtengerts and Rycroft, 2008), or at several other frequencies, including the upper and lower hybrid resonance frequencies. In the case of free electron masers (Ginzburg et al., 2002a) the emitted radiation is normally upshifted in frequency, depending on

how highly relativistic the electrons are.

Simulations in the laboratory usually need to be scaled because the laboratory dimensions are much smaller than those in the upper atmosphere, the ionosphere and the magnetosphere. Provided similar ratios of the most significant parameters are maintained, the laboratory simulations provide a realistic comparison with the naturally occurring phenomena that occupy much larger volumes (McConville et al., 2008; Ronald et al., 2011). Care needs to be taken in the design of the laboratory simulations and the interpretation of some interactions that do not lend themselves to straightforward scaling. Where, for example, an absolute threshold exists for a physical process, such as the particle energy thresholds that need to be exceeded for optical, X-ray and gamma ray production, the laboratory simulations are likely to need to be conducted in separate experimental regimes. Although the electric fields applied in the smaller dimensions of the laboratory simulations can be scaled up relative to those existing in the natural environment, the total electric potential differences experienced by the particles also need to result in accelerated particle energies that exceed the absolute thresholds for optical, X-ray and gamma ray production. In laboratory simulation experiments aimed primarily at simulating the generation of RF in the natural environment, it is therefore more difficult to simulate simultaneously the generation of all the shorter wavelength radiation emissions observed in the natural environment. By conducting the laboratory simulations in separately scaled regimes, ranging from the generation of non-ionizing (RF) radiation through to ionizing radiation (X-rays and gamma rays), it is possible to simulate each individual natural process and thereby provide an improved understanding of the naturally occurring phenomena. In laboratory simulations of RF generation the laboratory particle densities and any applied magnetic fields tend to be considerably higher in the laboratory experiments, which results in the relevant frequencies being greatly increased. For example the observed frequencies that are in the RF range in the natural environment tend to be typically scaled up into the microwave range in the laboratory simulations. This, however, results in the beneficial accompanying effect by which the wavelengths are correspondingly reduced and so the number of wavelengths that can fit within the smaller scale laboratory experiments is maintained sufficiently large so as to result in the same scale length to wavelength ratios that occur in the larger scale length natural phenomena. Examples of successful laboratory simulations of natural electron beam driven RF phenomena above the Earth's auroral regions have been reported (McConville et al., 2008; Ronald et al., 2011). The development of powerful computer codes and fast, large-memory computers has led to realistic numerical particle-in-cell (PiC) code simulations (Speirs et al., 2008; Gillespie et al., 2008) of both the natural phenomena and the laboratory-based relativistic electron beam experiments. In situations where the electron beam current is sufficiently high, it has been shown that narrowband RF radiation can be generated efficiently by a beam of relativistic electrons without requiring the normal resonant cavity structures (Ginzburg et al., 2002b), as a consequence

of the phenomenon of superradiance (Ginzburg et al., 1997; Yalandin et al., 2000).

The previous laboratory simulations and numerical modelling of discharges and electron beam interactions that have been cited herein have mainly contributed to a better understanding of electron beam driven auroral emission processes. The increasing use of a range of PiC codes supports laboratory experiments and the ability to model satellite observations of auroral kilometric radiation. It is suggested that relevant relativistic electron beam laboratory facilities and novel diagnostic experimental techniques would contribute importantly to a collaborative research programme on energetic charged particles and hard radiation above thunderclouds. This will support the aim of obtaining an improved understanding of the coupling processes between the Earth's atmosphere and near-Earth space that will be observed by the TARANIS research platform.

5.2 Observation of lightning discharges with spiral array

This section describes an efficient interferometric network geometry to map the electromagnetic emissions from lightning discharges and electron beams in two dimensions (compare with section 5.3).

The analysis of the electromagnetic radiation wave field recorded using a network with a structured geometric configuration and array processing techniques will allow the determination of the elevations and azimuths of atmospheric energetic events as well as the description of the time evolution and properties of the electromagnetic wave fields.

The array being considered as an integrated instrument as a whole, its transfer function $T_A(\mathbf{k})$ for a given topology $A_{distrib}(lon, lat)$ corresponds to the stack in the wave number space of an impulse source that propagates with an infinite velocity (zenithal incidence) over all the receivers $\mathbf{x}_p$ of the array

$$A_{\text{distrib}}(lon, lat) = \sum_{p=1}^{N_s} \delta(lon - lon_p)\delta(lat - lat_p), \tag{2}$$

$$T_A(\mathbf{k}) = \sum_{p=1}^{N_s} e^{i\mathbf{k}\mathbf{x}_p}, \quad \text{where} \quad \mathbf{x}_p = (lon_p, lat_p), \tag{3}$$

The separation ability of the array being defined by the half width of the central peak of $T_A(\mathbf{k})$. Taking into account the frequency band of the lightning discharges observed, i.e. from some tens to hundreds of kHz (Füllekrug et al., 2011b) we propose to spread an array of radio receivers made up of 14 individual antennas with a specific spiral geometry that avoids wave number aliasing

(Figure 9).

The wavelengths involved ranging from some km to tens of km will cross the array with apparent velocities between the speed of light c for horizontal incidence up to ∞ for zenithal incidence corresponding to wave numbers $2\pi/\lambda$ ranging from 0 to $10^{-3} - 10^{-4}$ rd.m^{-1}. A deterministic approximation of the lightning discharge allows the electromagnetic radiation to be modelled as a superposition of contributions (or components) $1 \leq j \leq N_c$ that arrive at a location $\mathbf{x}(lon, lat)$ at a given time t for each frequency f_i, $\quad 1 \leq i \leq N_f$; each contribution being characterized by its (horizontal) wave number $\mathbf{k}_{ij} = (k_{ij}^{lon}, k_{ij}^{lat})$ and amplitude $\varepsilon_{ij}(t)$ where η is additive noise

$$E(t, \mathbf{x}) = \sum_{i=1}^{N_f} \sum_{j=1}^{N_c} \varepsilon_{ij}(t) \times e^{i(\mathbf{k_{ij}x} - 2\pi f_i t + \phi_{ij}(t))} + \eta(t, \mathbf{x}). \tag{4}$$

As far as the signal processing techniques allow it, array analysis enables the signal to be decomposed into separate components, working in both wave number space and time-frequency space.

The back azimuth θ_{ij} and the apparent velocity c_{ij}^{app} of each component are determined with $\theta_{ij} = \tan^{-1}(k_{ij}^{lon}/k_{ij}^{lat})$ and $c_{ij}^{app} = 2\pi f_i / ||\mathbf{k}_{ij}||$, thus assuming a rectilinear propagation at the speed of light c_0, the zenithal angle of each source related to each component is determined as $\varphi_{ij} = \sin^{-1}(c_0/c_{ij}^{app})$. The response of the array to the wave field given in equation 4 is

$$R(t) = \sum_{p=1}^{N_s} \left(\sum_{i=1}^{N_f} \sum_{j=1}^{N_c} \varepsilon_{ij}(t) \times e^{i(\mathbf{k_{ij}x_p} - 2\pi f_i t + \phi_{ij}(t))} + \eta(t, \mathbf{x_p}) \right). \tag{5}$$

In the wave number space, eq. 5 corresponds to a Dirac distribution pointing to all $\mathbf{k}_{ij}$ convolved with $T_A(\mathbf{k})$ with amplitudes proportional to $\varepsilon_{ij}(t)$ (Figure 10). The emergence of these peaks in the frequency domain depends on the frequency content of $\varepsilon_{ij}(t)$. It becomes thus possible to deduce the information $(\theta_{ij}, \varphi_{ij}, f_i)$ and the time occurrences of the $\mathbf{k}_{ij}$ components using a global time-frequency-wave number analysis method (Delprat et al., 1992; Schisselé et al., 2004, 2005; Mallat, 2009) or time-frequency-wave number-polarization analysis using quaternion techniques (Le Bihan and Sangwine, 2003; Miron et al., 2006). Real time analysis could also be considered using techniques such as the Progressive Multiple Channel Correlation (Cansi, 1995).

The back azimuth accuracy is given by

$$\Delta\theta_{ij} = \cos(\theta) \times \sin(\theta) \left(\frac{\Delta k_x}{k_x} + \frac{\Delta k_y}{k_y} \right) \tag{6}$$

and the apparent velocity uncertainty by

$$\frac{\Delta C^{app}}{C^{app}} = \frac{\Delta f}{f} + \frac{\Delta ||\mathbf{k}||}{||\mathbf{k}||}. \tag{7}$$

The accuracy of C^{app} depends on $\frac{\Delta ||\mathbf{k}||}{||\mathbf{k}||}$ that may be constant considering a denser k sampling for the smaller values of k. In such a wavenumber sampling strategy, the accuracy $\Delta\theta$ and the uncertainty of C^{app} can reach a few degrees and a few percent respectively.

5.3 Radio remote sensing of upward relativistic electron beams

This section describes the radio remote sensing of electron beams above thunderclouds which may be detected with a sprial array (compare with section 5.2). The emitted electromagnetic radiation may be reproduced in the laboratory (compare with section 5.1) and can be detected at satellite altitudes (compare with section 5.4).

It is now well recognized that electric breakdown of air inside thunderclouds occurs at an ambient electric field strength of $\sim 10^5$ V/m at sea level which is $\sim$1 order of magnitude smaller than the conventional electric field breakdown threshold of air (Gurevich and Zybin, 2005; Marshall et al., 1995; Gurevich et al., 1992). This observation might be explained by a relativistic mechanism which requires energetic seed particles with energies above the runaway threshold of $\sim$10 keV or more (Lehtinen et al., 1999), dependent on the electric field strength present. Feedback mechanisms can assist to initiate a quickly growing electron avalanche (Dwyer et al., 2009; Dwyer, 2003) which radiates electromagnetic waves (Dwyer, 2012; Cummer et al., 2011; Gurevich et al., 2003). The seed particles could be secondary electrons from cosmic ray protons with primary energies of $\sim 10^{15}$–10^{16} eV (Gurevich and Zybin, 2005), but the diffusion of runaway electrons suggests that these seed particles from cosmic rays may not be sufficient (Dwyer, 2010). Alternatively, the seed particles could originate from thermal runaway electrons in leader and/or streamer tips (Celestin and Pasko, 2012, 2011; Moss et al., 2006). The avalanche of runaway electrons produces gamma ray photons with energies ranging from $\sim$1-100 MeV which are now routinely recorded on board spacecraft as terrestrial gamma ray flashes (Tavani et al., 2011; Smith et al., 2005; Fishman et al., 1994).

It was recently proposed that terrestrial gamma ray flashes (TGFs) of long duration may in fact be the detections of energetic electrons which propagated along the geomagnetic field line to the conjugate hemisphere (Dwyer et al., 2008). This novel interpretation is supported by the detection of transient narrow beams of relativistic electrons on board the SAMPEX spacecraft which are now denoted terrestrial electron flashes (Carlson et al., 2011, 2009).

A detailed reanalysis of terrestrial gamma ray flashes on the FERMI spacecraft established an unambiguous association with lightning discharges in the conjugate hemisphere which confirmed that the electrons indeed propagated along the geomagnetic field line to the spacecraft (Cohen et al., 2010). The coincident enhancement of the gamma ray spectrum at the positron annihilation line of 511 keV revealed that these electron beams are accompanied by positrons (Briggs et al., 2011) as predicted by (Dwyer et al., 2008).

Relativistic electron beams above thunderclouds emit bursts of low frequency electromagnetic waves which can be used to determine the physical parameters of electron beams by radio remote sensing (Roussel-Dupré et al., 1998; Roussel-Dupré and Gurevich, 1996). The predicted electromagnetic radiation of such electron beams has been detected by use of low frequency (LF) electromagnetic waves from ∼40–400 kHz which exhibit a relatively flat spectrum when compared with the spectrum of lightning discharges (Füllekrug et al., 2010). A detailed analysis shows that these radio signals tend to occur ∼2–9 ms after positive cloud-to-ground lightning discharges in agreement with the simulations. The lightning discharges deposit electromagnetic energy into the middle atmosphere which is subsequently partially discharged by electron beams and transient luminous events (compare with section 4.1). The electron beams occur at heights between ∼22–72 km above thunderclouds as inferred from the multipath propagation of the electromagnetic waves, i.e. a discrimination between the ground wave and the first hop sky wave reflected from the ionosphere. The numerical simulations suggest that the electron beams gain a mean energy of ∼7 MeV to transport a total charge of ∼-10 mC upwards within a downward impulsive current $\sim 3 \times 10^{-3}$ Am^{-2} (Füllekrug et al., 2011b). Note that these electron beams above thunderclouds currently appear to be very rare and that the energetic electrons and gamma rays escaping into near-Earth space remain to be detected by the TARANIS satellite which is specifically designed for simultaneous measurements of optical signatures from transient luminous events, electromagnetic waves, X- and gamma rays and energetic charged particles.

Future investigations of upward electron beams emanating from thunderclouds require a combination of observations on board the TARANIS satellite with sophisticated ground-based observations to constrain numerical simulations. The satellite needs to be able to distinguish between the energy deposition by terrestrial gamma ray flashes and terrestrial electron flashes, for example, by discriminating between their arrival directions. Simultaneous observations of electromagnetic waves on the ground need to cover a frequency range from some Hz up to tens of MHz to determine the complete radio spectrum generated by the electron beams. An interferometric array of radio receivers can map the radio sky (Figure 12) above thunderclouds, in order to obtain quantitative information on the charge transfer through the middle atmosphere. Extremely sensitive, high speed ∼1 μs optical imaging at UV wavelengths (e.g., ∼340 nm) may complement the radio recordings and help

to determine the spatial evolution of electron beams and their chemical impact on the neutral atmosphere.

5.4 Radio signatures of lightning and transient luminous events in space

This section describes the remote sensing of electromagnetic emissions from lightning discharges and transient luminous events on board of satellites. These measurements are also relevant for the detection of electron beams above thunderclouds (compare with section 5.3).

Ground-based observations of ELF/VLF atmospherics (sferics) have been extensively used for characterizing lightning discharges linked to transient luminous events. Such measurements allow the confirmation of sprite-causative cloud-to-ground flashes derived from lightning detection networks, and the characterization of the recorded waveforms in terms of their ELF slow-tail content (Reising et al., 1996) and charge transfer (Cummer and Inan, 2000). Due to the lack of data, ELF/VLF remote sensing of TLE causative lightning discharges from space is much less developed. Nevertheless, it is clear that information collected above the source regions may usefully complement observations made below them.

The first recording of satellite ELF/VLF waveform data associated with TLE observations was obtained during the DEMETER summer 2005 campaign. During that campaign TLEs were observed on the ground from Langmuir Laboratory in New Mexico, USA, and ELF/VLF waveform data were simultaneously recorded on board the satellite DEMETER and at Langmuir and Palmer station, Antarctica (Lefeuvre et al., 2009). However, because of the limitations of the operating modes and of the available scientific payload, only very few well-coordinated observations could be obtained. To overcome these limitations the French satellite TARANIS dedicated to the study of transient energy transfer processes known to occur above thunderstorms will have the capability to combine nadir optical observations of TLEs and high resolution wave field measurements over the frequency range DC - 35 MHz. By analysing these measurements it will be possible to obtain new information regarding the generation mechanisms. To achieve this aim it is necessary to disentangle the wave field perturbation due to the atmosphere-ionosphere propagation from the perturbation due to the transient luminous events (Füllekrug et al., 2011a).

From simulations performed using the IRI model for the ionospheric density profile and the Wait and Spies (1964) electron-collision profile, it can be shown that the transmission of ELF/VLF wave energy from the atmosphere to the ionosphere is performed through a complex k-filtering system which depends on the electron density profile at the bottom of the ionosphere (D and E regions), the electron-collision profile, and the wave frequency. From the DEMETER data it was also shown that thunderstorm-active regions and

VLF ground-based transmitters have a strong impact on the ionosphere above (Parrot et al., 2009). Consequently, to maximize the science return of the TARANIS mission, the modelling of the lower ionospheric layers and the characterization of the atmospheric conditions favouring the transfer of wave energy from the atmosphere to the ionosphere above thunderstorms are of prime interest.

6 Energetic charged particles and their impact on the Earth's atmosphere

Energetic charged particles impinging on the upper atmosphere result in ionization (6.1) which leads to perturbations of the ambient atmospheric chemistry which can be studied using various ground-based radio experiments (6.2). Upward and downward streaming energetic charged particles in the radiation belts (6.3) are affected by lightning discharges which need to be considered for spacecraft protection (6.4).

6.1 SuperDARN and energetic charged particles

This section describes the remote sensing of particle precipitation with SuperDARN, the relationship with the global atmospheric electric circuit (compare with section 2) and the possibility of detecting atmospheric gravity waves and particle precipitation above thunderstorms at mid latitudes which may be associated with electromagnetic emissions (compare with section 5.1) and perturbations of ambient atmospheric chemistry (compare with section 6.2).

The Super Dual Auroral Radar Network (SuperDARN) is an expanding network of HF coherent scatter radars whose primary aim has been to investigate the ionospheric flows in response to a range of different forcing conditions (for recent reviews see Chisham et al., 2007; Lester, 2008). The network began in 1995 with 6 radars in the northern hemisphere and 2 in the southern hemisphere while, at the start of 2012, there are 17 in the north and 8 in the south, with another 5 expected to be deployed in the north and 2 in the south in 2012. The radars were not originally designed to make measurements associated with either energetic particles or electric fields associated with thunderclouds in the geoelectric circuit. Nevertheless, there are certain observations which have been made which could supplement any new observations; these are outlined below.

Comparison of EISCAT measurements with SuperDARN radar spectra (Milan et al., 1999) demonstrated that the power in the radar spectrum could be enhanced by charged particle precipitation into the ionosphere associated with auroral arcs. In this study several events where the main peak of the SuperDARN radar spectrum was enhanced (e.g., Figure 11) were discussed. The

top three panels of Figure 11 illustrates one such event where the middle panel of the top row is the spectrum with enhanced power. Each of the three radar spectra in this row are normalised to the peak power in the middle spectrum and the two spectra on either side of this spectrum are those associated with low levels of electron density measured by EISCAT. In addition to the enhanced power there is also a secondary peak in the spectrum, with a negative Doppler velocity. The second row shows a similar example later in the period where the central panel again shows a significant enhancement, although on this occasion there is an additional peak with a larger positive Doppler velocity.

If there are significant fluxes of energetic charged particles coming upward from thunderclouds then it is anticipated that such spectral enhancements would be expected to be seen with the radars. The issue for the SuperDARN radars would be where the precipitation would cause enhanced electron density. If this occurs in the E-region, then signatures such as those shown in Figure 11 are likely while, if the electron density is enhanced in the D region, then the most likely effect will be the loss of the radar signal. This would be due to the enhanced signal absorption at the operational frequencies (Milan et al., 1999; Gauld et al., 2002). Such enhanced ionisation in the D-region due to lightning, specifically sprites and elves, has been established (Füllekrug and Rycroft, 2006).

In addition to particle precipitation there is also the possibility for a contribution to the geoelectric circuit (e.g., Roble, 1991). Recently comparisons between observations of the vertical component of the fair weather electric field at the ground at high latitudes and the SuperDARN estimates of the electric field above Hornsund have been made (Odzimek et al., 2011). In this study 31 fair weather days at Hornsund were identified between November 2004 and June 2009 and the ionospheric potential, estimated using the so-called map potential technique (Ruohoniemi and Baker, 1998), has been used. The comparison illustrates a clear correlation between the change in the vertical electric field at the ground (ΔE_{zn} in V/m) and the ionospheric potential (V_{conv} in V) which can be represented by the following empirical relationship $\Delta E_{zn} = 0.00094 \cdot V_{conv} + 0.0093$

Observations made by SuperDARN radars at high latitudes can therefore be used for the extraction of the ionospheric convection effects in the ground level geoelectric field from the field generated by electrified clouds globally. Furthermore, while this is the fair weather electric field, it is possible that any significant electric fields associated with thunderclouds could also be related in some way to the overhead ionospheric potential measured above thunderstorm areas.

While not directly related to the energetic charged particles associated with thunderstorms, SuperDARN may also be able to observe atmospheric gravity waves (AGWs) stimulated in the middle atmosphere by such thunderstorms.

These AGWs are most likely to break at the mesopause, but measurements of mesospheric winds by SuperDARN are possible (e.g., Hibbens et al., 2011) as are radar echoes which have similar annual occurrence distributions to polar mesosphere summer echoes, PMSE (e.g., Ogawa et al., 2003; Hosokawa et al., 2005). The AGWs caused by the thunderstorms may be visible in the variability of these observations.

With the extension of SuperDARN to mid-latitudes, in particular in the middle of continental USA, there is now a significant opportunity to make measurements of the ionospheric potential and the possible impact of energetic charged particles associated with thunderclouds. The radar modes may have to be chosen such that the radars operate at the highest time resolution and new modes of analysis will probably be required, but this opportunity forms the basis for further investigating the coupling from the middle atmosphere to the upper atmosphere.

6.2 Perturbations of ambient atmospheric chemistry

This section describes Riometer (cosmic noise absorption) measurements of particle precipitation (compare with section 6.1) which have an effect on the ambient upper atmosphere chemistry and which may be associated with electromagnetic emissons (compare with section 5.1).

Energetic charged particle precipitation is believed to have important effects on the chemistry of the middle atmosphere. In addition to the primary ionization produced by collisions between energetic particles and atmospheric constituents, much larger secondary ionization occurs because of interactions between the neutral atmosphere and the primary ionization products. These ionized species have energies in the range of a few hundred eV, which is more than sufficient to dissociate molecular nitrogen and to give rise to subsequent positive ion chemistry which dissociates water vapour. The result is the production of a number of odd hydrogen (HOx) and odd nitrogen (NOx) species at middle atmosphere altitudes from 20 to 100 km. NOx (N+NO+NO2) is a catalyst in the reaction that destroys atmospheric ozone (O3+NO $\rightarrow$ O2+NO2, O+NO2 $\rightarrow$ O2+NO) and is an efficient infrared radiator, making it important for the heat balance of the upper atmosphere. NOx has the potential to affect atmospheric dynamics, by directly altering temperature gradients in the mesosphere and stratosphere and via changes in the mesospheric boundary conditions for atmospheric circulation.

It is not clear which of these mechanisms operates or dominates; therefore it is vital to fully understand where NOx is produced, in what quantities, and where it is transported to. In a sunlit atmosphere odd nitrogen is lost via photo-dissociation by ultraviolet radiation. During the polar winter, the lifetime of NOx increases from days to months, making it subject to down-

ward transport by the polar vortex (Randall et al., 2001). Recent studies have shown that NOx transported into the polar stratosphere from the mesosphere can lead to as much as a 30 % loss of stratospheric ozone, lasting for 1 or 2 months (Seppälä et al., 2007). Recently Seppälä et al. (2009) confirmed the linkage between solar activity and substantial wintertime surface temperature variations in the polar regions. These impacts are significant in terms of natural polar temperature variability. Analysis suggests that the most likely mechanism connecting solar activity and surface temperature is the modification of the chemical composition of the upper atmosphere by energetic charged particle precipitation (Seppälä et al., 2009).

Direct estimates of the precipitating electrons can be gained from satellites, such as DEMETER or the upcoming TARANIS mission. However, due to the nature of their orbit, only snapshots of any given event can be obtained; having sufficient statistics of events can be used to provide empirical estimates. Although a perfectly valid technique, it cannot fully capture the dynamic nature of precipitation events. This issue can be addressed by supporting ground-based data such as Riometers (Relative Ionospheric Opacity Meters).

A Riometer is a sensitive radio receiver that records the cosmic radio noise in the high frequency (HF) band (Honary et al., 2011). These frequencies are strongly attenuated by increases of electron concentration in the lower ionosphere. The amount of absorption due to increased electron density can be determined by removing the known amount for a day of zero excess ionization (quiet day curve). For example, Riometers might be used in the future to study lightning induced particle precipitation (Inan et al., 2007), ionospheric modification by the lightning electromagnetic pulse (EMP) (Marshall, 2012) and thunderstorm generated gravity waves (Sentman et al., 2003; Jarvis et al., 2003). However, Riometers are particularly sensitive to electrons with energies from 10s to 100s of keV, which deposit mostly in the mesosphere. There are currently 11 imaging riometers and 58 wide-beam riometers located in the polar regions (polar cap and auroral zone) and, as such, they are ideally situated to study the very dynamic processes that govern the precipitation of energetic charged particles from the solar wind and magnetosphere into the upper atmosphere. Although riometers cannot directly measure either the flux or energy of the precipitating electrons, different techniques have been developed to provide estimates of these parameters, often via a combination with other diagnostics (Kosch et al., 2001). Kavanagh et al. (2004) compiled statistics from six years of data to demonstrate that electron precipitation at high latitudes was linked to variations in the solar wind, illustrating the important control that solar variability has over the coupling between the atmosphere and the near-Earth space environment.

The level of coupling between the solar wind and the Earth's magnetic environment depends on the level of geomagnetic activity which is normally

indicated by geomagnetic indices such as the three-hour Kp or daily Ap; however, these contain little (or no) information on location and the manner in which odd nitrogen is produced. For example, there are two principal energy/altitude regimes where NOx is produced via electron precipitation. Electrons with energy >100 keV ionize the atmosphere between ∼40 and 75 km altitude, whereas softer auroral electrons (1 keV - 10s of keV) deposit their energy into the height region of 80 to 120 km. The lack of detailed and continuous information on the precipitation spectra fundamentally reduces our ability to accurately estimate the formation of odd-nitrogen; there is still much to do to fully understand the variability and to gain a proper perspective on the importance of the processes involved.

6.3 Energetic charged particle observations on the DEMETER satellite

This section describes measurements of relativistic electrons on board the DEMETER satellite and their relation to the space environment with emphasis on stimulated particle precipitation into the Earth's atmosphere which can be triggered by transmitters and lightning discharges (compare with section 6.4).

On board the TARANIS spacecraft, the IDEE experiment aims to detect relativistic electrons related to Terrestrial Gamma-ray Flashes. A simpler detector with a moderate time resolution (1 or 4 seconds) was placed on board the DEMETER spacecraft, with an orbit quite similar to the planned orbit of TARANIS (Sauvaud et al., 2006). Several new results were obtained by DEMETER.

DEMETER data showed that geomagnetic storms are associated with the formation of multiple electron energy structures inside the inner radiation belt at L=1.1-1.8 and with proton energy bands located mainly inside the slot region at L=2.5-3.5. These structures, measured at energies higher than 150 keV and up to the MeV range result from the interaction of electrons and protons with quasi-monochromatic Ultra Low Frequency (ULF) waves in the 60-1000 second range induced by magnetospheric compressions under the effect of dense solar plasma and related injections of energetic charged particles from the outer magnetosphere which destabilize the field lines of the inner magnetosphere down to L=1.1. Using the low altitude polar orbiting DEMETER data, case studies and statistical studies of these energy structures were performed; they are best seen on the sides of the South Atlantic Anomaly where the mirror points of trapped radiation belt particles are lowered and reach the spacecraft. The structures are clearly correlated with geomagnetic activity and their association with quasi-monochromatic ULF waves was demonstrated. In particular, numerical simulations were used to show how global ULF waves drive the observed electron structures (Sauvaud et al., 2012).

The signals emitted by VLF navigation transmitters are observed in space as waves with a very narrow bandwidth. The effects of the VLF transmitter NWC in Australia on the inner radiation belt was studied using global observations at low altitudes. It was found that enhancements in the 100-600 keV drift-loss cone electron fluxes at L values between 1.4 and 1.7 are linked to NWC operation and to ionospheric absorption. Waves and particles moving in opposite directions interact in the vicinity of the magnetic equatorial plane. Using DEMETER passes across the drifting cloud of electrons caused by the transmitter, it was found that 300 times more 200 keV electrons are driven into the drift-loss cone during NWC transmission periods than during non-transmission periods. This results in an electron drift band encircling the Earth at L values around 1.7. The correlation between the flux of resonant electrons and the Dst index shows that the electron source intensity is controlled by magnetic storm activity (Sauvaud et al., 2008).

Other signals in the VLF range include lightning whistlers. The DEMETER spacecraft detects short bursts of lightning-induced electron precipitation (LEP) simultaneously with newly-injected upgoing whistlers, and sometimes also with once-reflected (from the conjugate hemisphere) whistlers. For the first time causative lightning discharges are definitively geo-located for some LEP bursts on board a satellite. The LEP bursts occur within <1 s of the causative lightning and consist of 100-300 keV electrons. First in situ observations of large regions of enhanced background precipitation were detected (Inan et al., 2007). The regions are apparently produced and maintained by a high rate of lightning within a localized thunderstorm. Furthermore, the analysis of the DEMETER spacecraft particle data shows that energetic electron precipitation exhibits a seasonal dependence consistent with lighting-induced electron precipitation (LEP). Over the USA, energetic electron fluxes in the slot region (between L=2 and 3) are significantly higher in the northern summer than in the winter, consistent with the seasonal variation of lightning activity in the northern hemisphere. The association of precipitating fluxes with lightning was explored using lightning location data from the National Lightning Detection Network (NLDN) and VLF wave data on DEMETER. The increased precipitation of charged particles into the drift loss cone over the northern hemisphere in summer is consistent with the expected pitch-angle scattering by lightning-generated whistler waves, indicating that lightning is a significant contributor to the loss of electrons in the slot region (Gemelos et al., 2009; Inan et al., 2007).

6.4 Lightning effects on the radiation belts

This section describes the behavior of relativistic particles in the space environment, the influence of transmitters and lightning discharges on the particle populations in the radiation belts (compare with section 6.3) and the corre-

sponding impact of energetic particles on satellites.

In the early 1960s, the USA and the USSR conducted a series of high altitude nuclear detonations (HAND). One of the results of these experiments was the injection of high energy electrons up to several MeV into the Earth's radiation belts, mainly in the region between L ∼1.2-2.5 (Hess, 1963) which became trapped in the Earth's magnetic field. Electrons below L=1.3 were quickly removed by Coulomb collisions with the atmosphere, but at higher L-values, although the lifetime of trapped electrons was much longer, typically a year near L=1.5, the decay rate was much higher than that due to collisions alone (Walt, 1964). It was quickly established that precipitation due to wave-particle interactions in the magnetosphere was responsible, and later that wave-particle interactions are responsible for the slot region between the inner and outer radiation belt (Lyons et al., 1972). These HAND experiments provided the first experimental proof that wave-particle interactions are a major electron loss process in space.

It is now known that there are several different types of waves that can contribute to electron loss from the radiation belts (Abel and Thorne, 1998). Plasmaspheric hiss reduces the loss timescale, i.e. the time for the trapped particle population to decay by a factor of 2.718, mainly in the outer plasmasphere out to the plasmapause which is usually located near L=4. At lower L-values a fraction of the electromagnetic radiation arising from lightning is able to escape into space and reduce the lifetime of trapped electrons of 0.5 MeV in the region L=2.0-3.6. Much closer to the Earth, between L ∼1.3-2.5 radio waves from ground-based VLF transmitters, used for communicating with submarines and until recently for navigation, appears to be the most effective source of waves for removing energetic electrons, as mentioned in the previous sub-section. The work of Abel and Thorne (1998) remains one of the most important and comprehensive studies of electron loss rates due to different types of waves, but it is based on a number of assumptions. These include the amount of wave power that can be transmitted through the ionosphere and escape into space, both from lightning and ground-based transmitters (Starks et al., 2008, 2009), how the power is distributed in local time, and the lightning flash rate. These assumptions are critical for determining the electron loss timescale, and which waves dominate where.

Recent observations have confirmed that VLF transmitters cause electron loss (Sauvaud et al., 2008) which could be used to precipitate electrons into the upper atmosphere (Inan et al., 2003). However, electron loss rates due to naturally produced waves such as plasmapsheric hiss depend on geomagnetic activity (Meredith et al., 2009; Baker et al., 2007). Using wave data from the CRRES satellite electron loss timescales due to lightning generated whistlers were found to be as low as 10-20 days for 2 MeV electrons near L=2 for (Meredith et al., 2009). These calculations depend critically on the measured wave power and the direction of propagation of the waves. As the

waves emerge from the ionosphere the wave normal angle is initially small due to ionospheric transmission conditions (Helliwell, 1965) but ray tracing shows that it increases to 50 degrees or so on the first pass across the magnetic equator (Thorne and Horne, 1994). However, if the waves are guided by a density gradient the wave normal angle can remain small along the propagation path which increases scattering and reduces the loss timescale significantly. Thus lightning generated whistlers may be far more important in removing electrons from the radiation belts than ground based transmitter signals over a wide range of L shells.

Satellites such as DEMETER have been able to measure the radio wave power above the ionosphere, and to measure electron precipitation. However, the data have been restricted in latitudinal coverage; the amount of high resolution burst mode data was severly restricted. A new satellite mission with a larger latitudinal coverage that includes the outer radiation belt and with the ability to capture the short duration burst precipitation characteristic of wave-particle interactions due to lightning generated whistlers is required. Burst precipitation may well be the dominant form of electron loss (Thorne et al., 2005), but apart from lightning generated whistlers it could also arise from natural wave emissions such as chorus and electromagnetic ion cyclotron waves. The relative contributions from these three processes have yet to be established. Furthermore, the type of wave-particle interaction involved, with high amplitude short duration bursts, is inherently nonlinear (Trakhtengerts and Rycroft, 2008). Calculating the true loss rates requires a challenging study in nonlinear plasma physics for a regime that is not easily accessible in the laboratory.

Changes in the space radiation environment are a part of space weather and pose a risk to satellites on orbit. Each satellite is designed to withstand the nominal radiation environment in which it will orbit. However, a severe space weather event or a high altitude nuclear detonation can increase radiation levels by orders of magnitude. Understanding the extent to which lightning generated whistlers can remove the radiation, how long it would take, and the location and particle energies that would be removed is a challenging, but strategically important scientific question.

7 Summary

Society increasingly relies on sensitive automated technological systems, both in space and elsewhere. One of the grand challenges of our time is to ensure that technological systems operate securely, in particular for safety critical applications. The French Embassy in London brought together a Franco-British team of world leading experts to discuss recently discovered energetic charged particles and hard radiation in the Earth's atmosphere and their impact on technological systems, e.g., the TARANIS satellite. The TARANIS satellite is

a novel asset of the French government which represents a total investment of ∼50 million Euro and ∼200 man-years. The scientists reviewed and assessed the current state of scientific knowledge which ranged from laboratory plasma physics to plasmas in the natural environment and the design of the French satellite TARANIS. Based on this assessment, the expert panel formulated one fundamental key science question to push forward the boundaries of knowledge on energetic processes and their impact on the Earth's atmosphere:

What are the causes and consequences of relativistic charged particle beams in atmospheric environments?

This key science question breaks down into a set of more specific key science questions which have been identified by the expert panel to take forward this research area:

1. How do transient energetic charged particle ensembles behave in atmospheric environments?
2. What are the properties of relativistic particle beams in the Earth's atmosphere?
3. How do aerosols and dust charge contribute to the acceleration of particles and affect atmospheric electric circuits?
4. How can transient luminous events and terrestrial gamma ray flashes be used as a plasma diagnostic?
5. What are the impacts of relativistic particle ensembles and radiation?
6. What is the broader significance of relativistic charged particles in atmospheric environments?

Answering these key science questions in such a highly dynamic research area is a grand challenge. Therefore, the expert panel decided to initiate a collaborative framework to address the above questions in future well-coordinated international research programs. These international research programs are intended to complement the capital investment ∼150 million Euros of governments around the world in six forthcoming space missions (ASIM, CHIBIS, FireFly, GLIMS, RISING2 and TARANIS) to unravel the mysteries of energetic processes in the Earth's atmosphere. For example, the Russian microsatellite Chibis was launched in January, 2012, whilst others space mission are awaiting their launch opportunity, are currently being built or are in preparation. It is thought that answering these key science questions will clarify the physics of energetic processes in the Earth's atmosphere and their impact on technological systems and the Earth's climate on which today's society relies.

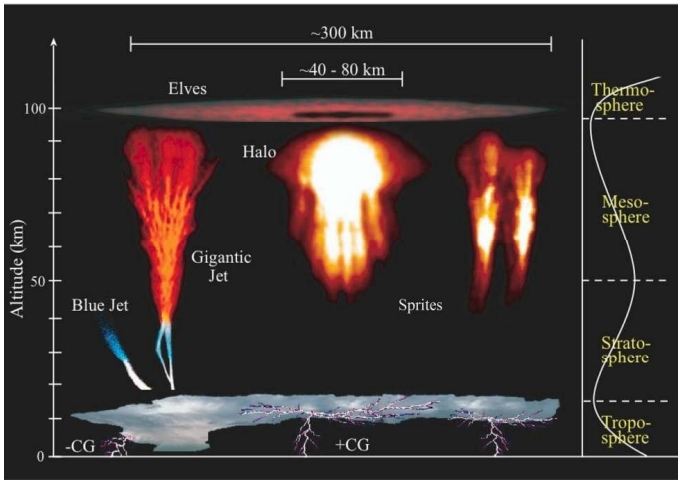

Fig. 1 Transient luminous events above thunderclouds are denoted blue jets, gigantic jets, sprite halos, sprites, and elves (courtesy M. Sato).

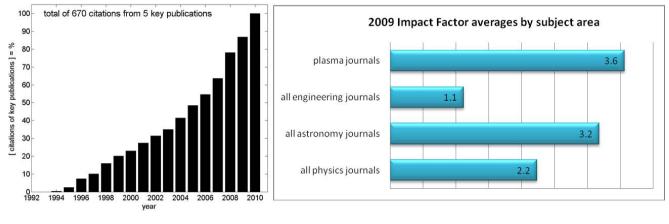

Fig. 2 Left. The number of citations of key publications on energetic processes above thunderclouds currently experiences an exponential increase which is predicted to accelerate as the planned space missions approach their launch (courtesy M. Füllekrug). **Right.** Plasma physics journals exhibit very high impact factors (courtesy D. Diver).

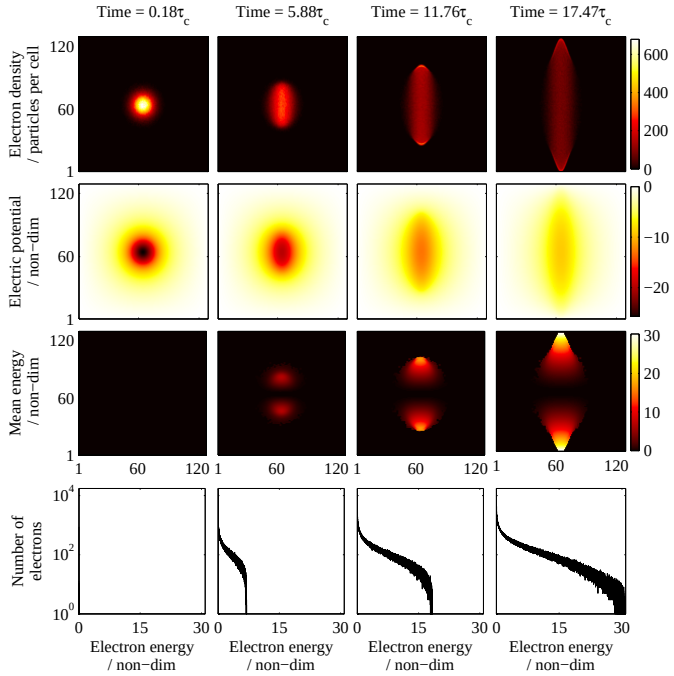

Fig. 3 Expansion of an initially spherical cloud of electrons in a vertical magnetic field. Top row shows the spatial distribution of electron density as time evolves (left-to-right sequence), with the characteristic time τ_c being the electron cyclotron period. Second row shows the evolution of the (self) electric potential; third row: the mean electron energy; bottom row: the electron energy distribution function evolution. Note that the most energetic electrons are located at the tips of the expansion along the magnetic field, and have reached energies that exceed the initial maximum electric potential at $t = 0$. More details can be found in (MacLachlan et al., 2009).

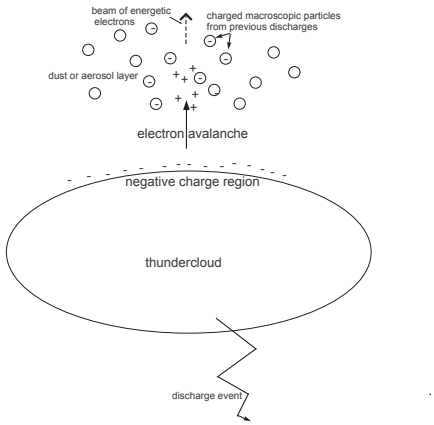

Fig. 4 An electron avalanche caused by ejection of electrons from the thundercloud top is injected into a pre-existing distribution of positive and negative charge, that constrains the spatial evolution of the upward jet, and boosts the energy of the leading electrons by virtue of harnessing the electrostatic field of the previous event. Electrons from the previous discharge are attached to dust or aerosols, and so dissipate much more slowly than the free electron diffusion rate.

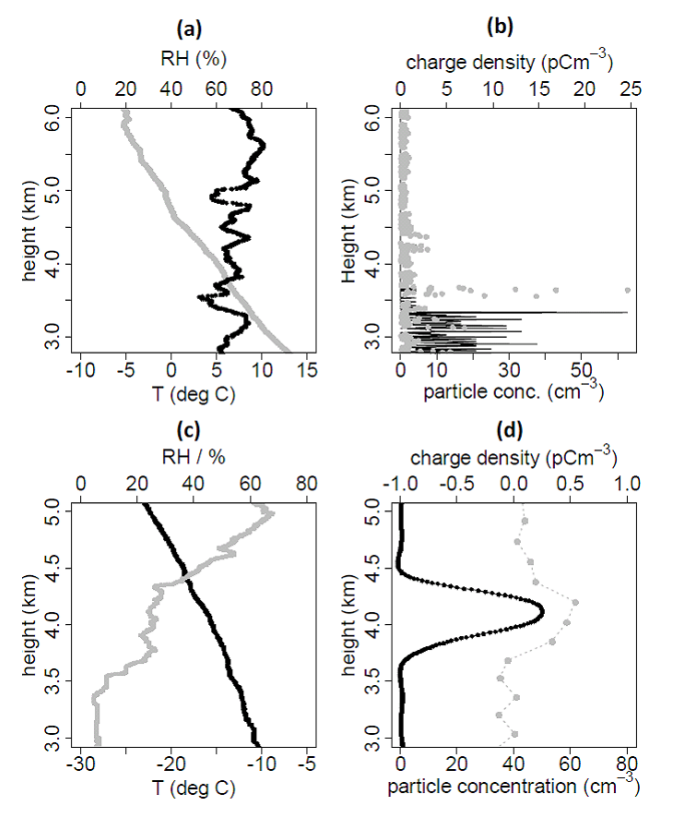

Fig. 5 Vertical profiles from balloon borne instruments through an elevated layer of Saharan dust over the Cape Verde isles ((a) and (b) taken from Nicoll et al. (2011)), and a volcanic ash plume over Scotland ((c) and (d), adapted from Harrison et al. (2010)). (b) and (d) show particle number concentration (black) and charge density (grey) measured by a disposable balloon borne aerosol counter and space charge sensor respectively. (a) and (c) show meteorological profiles of temperature (T, grey) and relative humidity (RH, black) to demonstrate that the particle and charge measurements are not related to the environmental conditions in which the sensors operate, and in particular that no liquid water cloud is present.

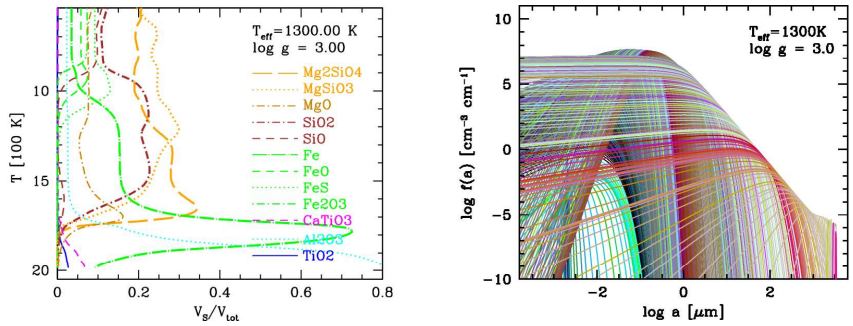

Fig. 6 Material composition (left) in units of volume fractions $V_{\rm s}/V_{\rm tot}$ and grain size distributions $f(a, z)$ (right) across the cloud layer increments z for a planetary object with an effective temperature of $T_{\rm eff}$ = 1300K and log(g)=3.0.

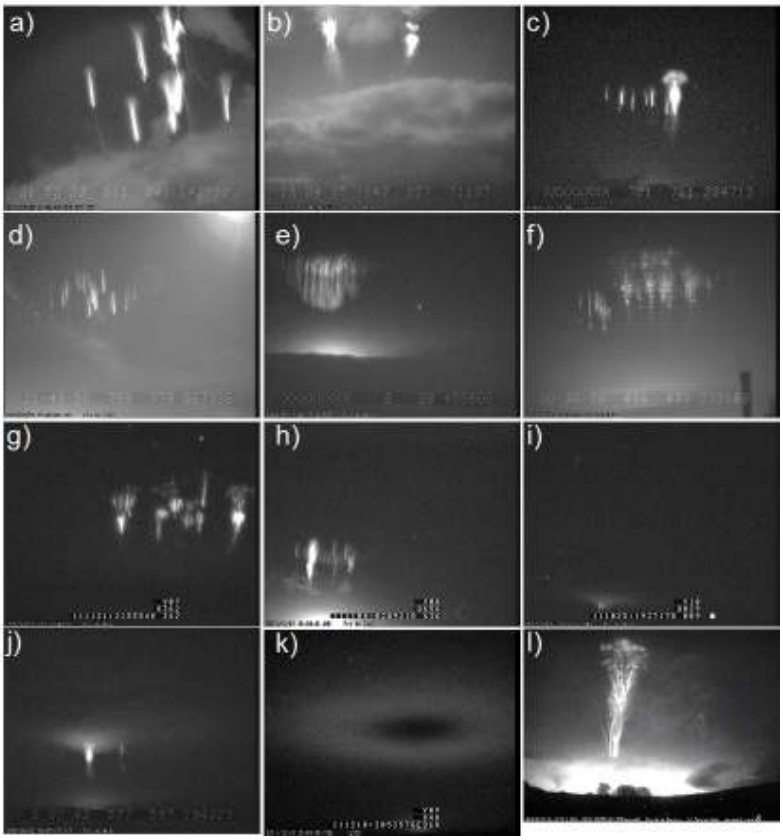

Fig. 7 Images of TLEs in 20 ms frames issued from video imagery: a) Column sprite elements above a storm at about 150 km from the camera. b) Carrot sprites at a different development stage, triggered by the same CG flash located at about 200 km from the camera. c) Group of column sprite elements with a jellyfish sprite in the foreground (∼300 km from the camera). d) Group of column sprites at about 300 km from the camera. e) Group of sprite elements with very developed tendrils (at 320 km from the camera). f) and g) Kind of dancing sprites (at 190 and 260 km from the camera, respectively). h) Group of circular-organized and bended sprite elements (at 380 km from the camera). i) Remote carrot sprite with halo (880 km from the camera). j) Carrot sprite centred below a halo and column element (390 km from the camera). k) Elve above a CG flash located at 340 km from the camera. l) Gigantic jet at the fully developed stage (∼50 km from the camera in Reunion Island).

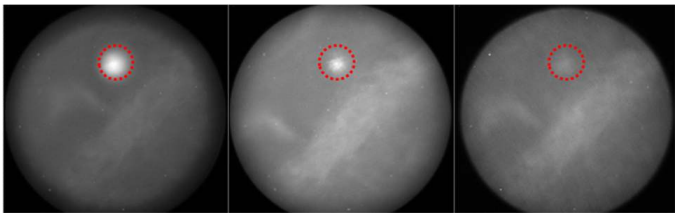

Fig. 8 Images of radio wave induced optical emissions in the F-region ionosphere from EISCAT on 20 November 2011 14:32-33 UT. From left to right, 630, 557.7 and 844.6 nm corresponding to electron energy thresholds of approximately 2, 4.2 and 11 eV. The image field of view is $\sim 50^{o}$ pointing vertically. The red circle denotes the pump beam mapped up to $\sim$250 km altitude. Other features outside the pump beam are stars and clouds.

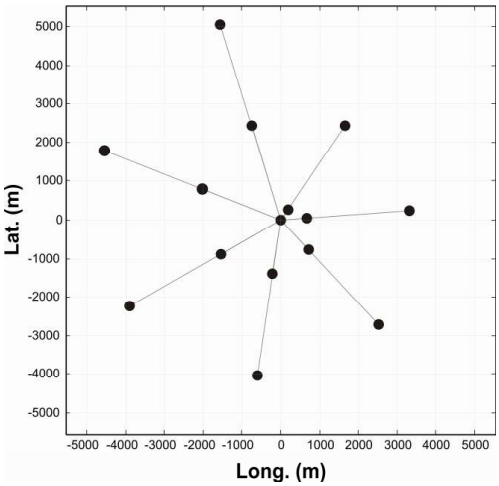

Fig. 9 Example of spiral array geometry with inner distances ranging from 0.3 to 9.2 km.

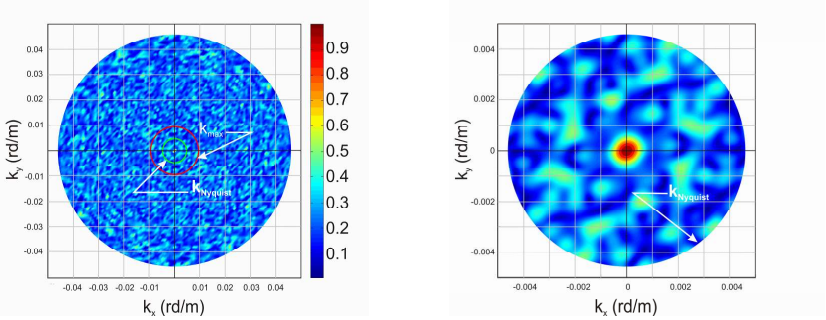

Fig. 10 Left. Wavenumber transfer function extended to 10 times the Nyquist wavenumber (green circle). **Right.** Zoom within the Nyquist area. The width at half maximum is $\sim 4 \times 10^{-4}$ rd.m^{-1} for the array with an extension of 10 km and reaches $\sim 2 \times 10^{-4}$ rd.m^{-1} with an extension of 20 km.

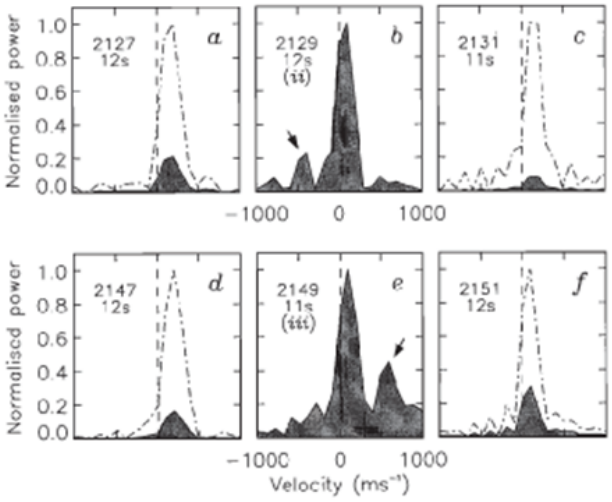

Fig. 11 The top three panels represent consecutive radar spectra from the Hankasalmi SuperDARN radar for a specific range gate which is located over the EISCAT radar. The central panel occurs at a time when there is significant ionisation caused by particle precipitation into the ionosphere resulting in enhanced power in the radar spectrum. The bottom three panels show three consecutive radar spectra for a second such precipitation event.

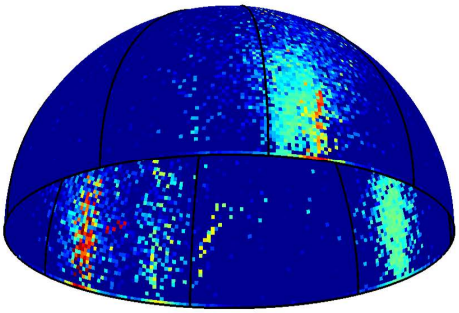

Fig. 12 Map of the 100 kHz radio sky on May 13, 2011, 15:00 UTC, recorded with an interferometric network of ten radio receivers distributed over $\sim$1 km^2 on Charmy Down airfield near Bath in South West England of the UK. The logarithm of small energies are depicted by blue/green/yellow colours and large energies are depicted in red. The small energies are related to the LOng RAnge aid to Navigtation (LORAN) transmitters in Lessay, Soustons, Anthorn and Rantum. The large energies to the left are related to an unknown event, possibly a lightning discharge.

Acknowledgements This review was prepared for a meeting at the French Embassy in London, November 17-18, 2011, to establish a novel Franco-British collaboration centred on the satellite TARANIS. The invitees are grateful to the French Embassy for sponsoring and hosting this meeting in the most professional way. MF is supported by the Natural Environment Research Council (NERC) under grant NE/H024921/1, ADRP is supported by the EPSRC under grant EP/G04239X/1. ChH acknowledges an ERC starting grant from the European Union.

References

Abel, B. and Thorne, R.: Electron scattering loss in Earth's inner magnetosphere 1. Dominant physical processes, Journal of Geophysical Research, 103, 2385–2396, doi:10.1029/97JA02919, 1998.

Allen, J. and Phelps, A.: Waves and microinstabilities in plasmas - linear effects, Reports on Progress in Physics, 40, 1305–1368, doi:10.1088/0034-4885/40/11/002, 1977.

Babich, L., Donskoy, E., Kutsyk, I., and Roussel-Dupré, R.: Characteristics of a relativistic electron avalanche in air, Doklady Physics, 49, 35–38, doi:10.1134/1.1648089, 2004.

Baker, D., Kanekal, S., Horne, R., Meredith, N., and Glauert, S. A.: Low-altitude measurements of 26 MeV electron trapping lifetimes at $1.5 \leq L \leq 2.5$, Geophysical Research Letters, 34, doi:10.1029/2007GL031007, 2007.

Barrington-Leigh, C., Inan, U., and Stanley, M.: Identification of sprites and elves with intensified video and broadband array photometry, Journal of Geophysical Research, 106, 1741–1750, doi:10.1029/2000JA000073, 2001.

Becker, K., Schoenbach, K., and Eden, J.: Microplasmas and applications, Journal of Physics D: Applied Physics, 39, R55–R70, doi:10.1088/0022-3727/39/3/R01, 2006.

Blanc, E., Farges, T., Roche, R., Brebion, D., Hua, T., Labarthe, A., and Melnikov, V.: Nadir observations of sprites from the International Space Station, Journal of Geophysical Research, 109, 1–8, doi:10.1029/2003JA009972, 2004.

Blanc, E., Farges, T., Brebion, D., Labarthe, A., and Melnikov, V.: Observations of sprites at the nadir; The LSO (Lightning and Sprite Observations) experiment on board of the International Space Station, in: Sprites, Elves and Intense Lightning Discharges, edited by Füllekrug, M., Mareev, E., and Rycroft, M., vol. NATO Science Series II, 225, Springer, Dordrecht, The Netherlands, 2006.

Blanc, E., Lefeuvre, F., Roussel-Dupré, R., and Sauvaud, J.: TARANIS: A microsatellite project dedicated to the study of impulsive transfers of energy between the Earth atmosphere, the ionosphere, and the magnetosphere, Advances in Space Research, 40, 1268–1275, doi:10.1016/j.asr.2007.06.037, 2007.

Boccippio, D., Williams, E., Heckman, S., Lyons, W., Baker, I., and Boldi, R.: Sprites, ELF transients, and positive ground strokes, Science, 269, 1088–1091, doi:10.1126/science.269.5227.1088, 1995.

Boeck, W., Vaughan, O., Blakeslee, R., Vonnegut, B., and Brook, M.: Lightning induced brightening in the airglow layer, Geophysical Research Letters, 19, 99–102, doi:10.1029/91GL03168, 1992.

Bonaventura, Z., Bourdon, A., Celestin, S., and Pasko, V.: Electric field determination in streamer discharges in air at atmospheric pressure, Plasma Sources Science and Technology, 20, doi:10.1088/0963-0252/20/3/035012, 2011.

Briggs, M., Connaughton, V., Wilson-Hodge, C., Preece, R., Fishman, G., Kippen, R., Bhat, P., Paciesas, W., Chaplin, V., Meegan, C., von Kienlin, A., Greiner, J., Dwyer, J., and Smith, D.: Electron-positron beams from terrestrial lightning observed with Fermi GBM, Geophysical Research Letters, 38, 1–5, doi:10.1029/2010GL046259, 2011.

Bryers, C., Kosch, M., Senior, A., Rietveld, M., and Yeoman, T.: EISCAT observations of pump-enhanced plasma temperature and optical emission excitation rate as a function of power flux, Journal of Geophysical Research, 117, 1–12, doi:10.1029/2012JA017897, 2012.

Cansi, Y.: An automatic seismic event processing for detection and location: the P.M.C.C method, Geophysical Research Letters, 22, 1021–1024, doi: 10.1029/95GL00468, 1995.

Carlson, B., Lehtinen, N., and Inan, U.: Observations of terrestrial gamma-ray flash electrons, in: Coupling of thunderstorms and lightning discharges to near-Earth space, edited by Crosby, N., Huang, T., and Rycroft, M., pp. 84–91, American Institute of Physics, Melville, 2009.

Carlson, B., Gjesteland, T., and Østgaard, N.: Terrestrial gammaray flash electron beam geometry, fluence, and detection frequency, Journal of Geophysical Research, 116, 1–7, doi:10.1029/2011JA016812, 2011.

Celestin, S. and Pasko, V.: Effects of spatial non-uniformity of streamer discharges on spectroscopic diagnostics of peak electric fields in transient luminous events, Geophysical Research Letters, 37, 1–15, doi: 10.1029/2010JA016260, 2010.

Celestin, S. and Pasko, V.: Energy and fluxes of thermal runaway electrons produced by exponential growth of streamers during the stepping of lightning leaders and in transient luminous events, Journal of Geophysical Research, 116, 1–14, doi:10.1029/2010JA016260, 2011.

Celestin, S. and Pasko, V.: Compton scattering effects on the duration of terrestrial gamma ray flashes, Journal of Geophysical Research, 39, 1–9, doi:10.1029/2011GL050342, 2012.

Chanrion, O. and Neubert, T.: Production of runaway electrons by negative streamer discharges, Journal of Geophysical Research, 115, doi: 10.1029/2009JA014774, 2010.

Chisham, G., Lester, M., Milan, S., Freeman, M., Bristow, W., Grocott, A., MacWilliams, K., Ruohoniemi, J., Yeoman, T., Dyson, P., Greenwald, R., Kikuchi, T., Pinnock, M., Rash, J., Sato, N., Sofko, G., Villain, J., and Walker, A.: A decade of the Super Dual Auroral Radar Network (SuperDARN): Scientific achievements, new techniques and future directions, Surveys in Geophysics, 28, 33–109, doi:10.1007/s10712-007-9017-8, 2007.

Cohen, M., Inan, U., Said, R., Briggs, M., Fishman, G., Connaughton, V., and Cummer, S.: A lightning discharge producing a beam of relativistic electrons into space, Geophysical Research Letters, 37, 1–4, doi: 10.1029/2010GL044481, 2010.

Cummer, S. and Inan, U.: Modeling ELF radio atmospheric propagation and extracting lightning currents from ELF observations, Radio Science, 35, 385–394, doi:10.1029/1999RS002184, 2000.

Cummer, S., Lu, G., Briggs, M., Connaughton, V., Xiong, S., Fishman, G., and Dwyer, J.: Geophysical Research Letters, 38, 1–6, doi: 10.1029/2011GL048099, 2011.

De Larquier, S. and Pasko, V.: Mechanism of inverted−chirp infrasonic radiation from sprites, Geophysical Research Letters, 37, 1–5, doi: 10.1029/2010GL045304, 2010.

Delprat, N., Escudié, B., Guillemain, P., Kronland-Martinet, R., Tchamitchian, P., and Torrésani, B.: Asymptotic wavelet and Gabor analysis: extraction of instantaneous frequencies, IEEE Transactions on Information Theory, 38, 644–664, doi:10.1109/18.119728, 1992.

Desch, S. and Cuzzi, J.: The generation of lightning in the solar nebula, Icarus, 143, 87–105, doi:10.1006/icar.1999.6245, 2000.

Dowds, B., Barrett, R., and Diver, D.: Streamer initiation in atmospheric pressure gas discharges by direct particle simulation, Physical Review E, 68, doi:10.1103/PhysRevE.68.026412, 2003.

Dwyer, J.: A fundamental limit on electric fields in air, Geophysical Research Letters, 30, 2055–2058, doi:10.1029/2003GL017781, 2003.

Dwyer, J.: Diffusion of relativistic runaway electrons and implications for lightning initiation, Journal of Geophysical Research, 115, 1–11, doi: 10.1029/2009JA014504, 2010.

Dwyer, J.: The relativistic feedback discharge model of terrestrial gamma ray flashes, Journal of Geophysical Research, 117, 1–25, doi: 10.1029/2011JA017160, 2012.

Dwyer, J., Grefenstette, B., and Smith, D.: High-energy electron beams launched into space by thunderstorms, Geophysical Research Letters, 35, 1–5, doi:10.1029/2007GL032430, 2008.

Dwyer, J., Uman, M., and Rassoul, H.: Remote measurements of thundercloud electrostatic fields, Journal of Geophysical Research, 114, 1–19, doi: 10.1029/2008JD011386, 2009.

Dwyer, J., Smith, D., and Cummer, S.: High-energy atmospheric physics: Terrestrial gamma-ray flashes and related phenomena, Space Science Reviews, 167, 1–64, doi:10.1007/s11214-012-9894-0, 2012.

Ebert, U., Nijdam, S., Li, C., Luque, A., Briels, T., and van Veldhuizen, E.: Review of recent results on streamer discharges and their relevance for sprites and lightning, Journal of Geophysical Research, 115, doi: 10.1029/2009JA014867, 2010.

Farges, T. and Blanc, E.: Characteristics of infrasound from lightning and sprites near thunderstorm areas, Journal of Geophysical Research, 115, doi: 10.1029/2009JA014700, 2010.

Farges, T., Blanc, E., Pichon, A. L., Neubert, T., and Allin, T.: Identification of infrasound produced by sprites during the Sprite2003 campaign, Geophysical Research Letters, 32, 1–4, doi:10.1029/2004GL021212, 2005.

Farrell, W. and Desch, M.: Cloud-to-stratosphere lightning discharges: A radio emission model, Geophysical Research Letters, 19, 665–668, doi: 10.1029/91GL02955, 1992.

Fishman, G., Bhat, P., Mallozzi, R., Horack, J., Koshut, T., Kouveliotou, C., Pendleton, G., Meegan, C., Wilson, R., Paciesas, W., Goodman, S., and Christian, H.: Discovery of intense gamma-ray flashes of atmospheric origin, Science, 264, 1313–1316, doi:10.1126/science.264.5163.1313, 1994.

Franz, R., Nemzek, R., and Winckler, J.: Television image of a large upward electrical discharge above a thunderstorm system, Science, 249, 48–51, doi: 10.1126/science.249.4964.48, 1990.

Fridman, A., Chirokov, A., and Gutsol, A.: Non-thermal atmospheric pressure discharges, Journal of Physics D: Applied Physics, 38, 1–24, doi: 10.1088/0022-3727/38/2/R01, 2005.

Fukunishi, H., Takahashi, Y., Kubota, M., Sakanoi, K., Inan, U., and Lyons, W.: Elves: Lightning-induced transient luminous events in the lower ionosphere, Geophysical Research Letters, 23, 2157–2160, doi: 10.1029/96GL01979, 1996.

Füllekrug, M. and Rycroft, M.: The contribution of sprites to the global atmospheric electric circuit, Earth, Planets and Space, 58, 1193–1196, 2006.

Füllekrug, M., Mareev, E., and Rycroft, M., eds.: Sprites, Elves and Intense Lightning Discharges, Springer, Dordrecht, 2006.

Füllekrug, M., Roussel-Dupré, R., Symbalisty, M., Chanrion, O., Odzimek, A., van der Velde, O., and Neubert, T.: Relativistic runaway breakdown in low frequency radio, Journal of Geophysical Research, 115, 1–10, doi: 10.1029/2009JA014468, 2010.

Füllekrug, M., Hanuise, C., and Parrot, M.: Experimental simulation of satellite observations of 100 kHz radio waves from relativistic electron beams above thunderclouds, Atmospheric Chemistry and Physics, 11, 1–7, doi: 10.5194/acp-11-1-2011, 2011a.

Füllekrug, M., Roussel-Dupré, R., Symbalisty, E., Colman, J., Chanrion, O., Soula, S., van der Velde, O., Odzimek, A., Bennett, A., Pasko, V., and Neubert, T.: Relativistic electron beams above thunderclouds, Atmospheric Chemistry and Physics, 11, 7747–7754, doi:10.5194/acp-11-7747-2011, 2011b.

Gauld, J., Yeoman, T., Davies, J., Milan, S., and Honary, F.: SuperDARN radar HF propagation and absorption response to the substorm expansion phase, Annales Geophysicae, 20, 1631–1645, doi:10.5194/angeo-20-1631-2002, 2002.

Gemelos, E., Inan, U., Walt, M., Parrot, M., and Sauvaud, J.: Seasonal dependence of energetic electron precipitation: evidence for a global role of lightning, Geophysical Research Letters, 36, 1–5, doi:10.1029/2009GL040396, 2009.

Gillespie, K., Speirs, D., Ronald, K., McConville, L., Phelps, A., Bingham, R., Cross, A., Robertson, C., Whyte, C., He, W., Vorgul, I., Cairns, R., and Kellett, B.: 3D PiC code simulations for a laboratory experimental investigation of Auroral Kilometric Radiation mechanisms, Plasma Physics and Controlled Fusion, 50, doi:10.1088/0741-3335/50/12/124038, 2008.

Ginzburg, N., Sergeev, A., Zotova, I., Novozhilova, Y., Peskov, N., Konoplev, I., Phelps, A., Cross, A., Cooke, S., Aitken, P., Shpak, V., Yalandin, M.,

Shunailov, C., and Ulmaskulov, M.: Experimental observation of superradiance in millimeter-wave band, Nuclear instruments and methods in physics research section A - accelerators, spectrometers, detectors and associated equipment, 393, 352–355, doi:10.1016/S0168-9002(97)00509-3, 1997.

Ginzburg, N., Peskov, N., Sergeev, A., Konoplev, I., Cross, A., Phelps, A., Robb, G., Ronald, K., He, W., and Whyte, C.: Theory of free-electron maser with two-dimensional distributed feedback driven by an annular electron beam, Journal of Applied Physics, 92, 1619–1629, doi:10.1063/1.1481193, 2002a.

Ginzburg, N., Peskov, N., Sergeev, A., Phelps, A., Cross, A., and Konoplev, I.: The use of a hybrid resonator consisting of one-dimensional and two-dimensional Bragg reflectors for generation of spatially coherent radiation in a coaxial free-electron laser, Physics of Plasmas, 9, 2798–2802, doi:10.1063/1.1476664, 2002b.

Gurevich, A. and Zybin, K.: Runaway breakdown and the mysteries of lightning, Physics Today, 58, 37–43, doi:10.1063/1.1995746, 2005.

Gurevich, A., Milikh, G., and Roussel-Dupré, R.: Runaway electron mechanism of air breakdown and preconditioning during a thunderstorm, Physics Letters A, 165, 463–468, doi:10.1016/0375-9601(92)90348-P, 1992.

Gurevich, A., Duncan, L., Karashtin, A., and Zybin, K.: Radio emission of lightning initiation, Phys. Lett. A, 312, 228–237, doi:10.1016/S0375-9601(03)00511-5, 2003.

Gustavsson, B., Sergienko, T., Kosch, M., Rietveld, M., Brändström, B., Leyser, T., Isham, B., Gallop, P., Aso, T., Ejiri, M., Grydeland, T., LaHoz, C., Kaila, K., Jussila, J., and Holma, H.: The electron energy distribution during HF pumping, a picture painted with all colors, Annales Geophysicae, 23, 1747–1754, doi:10.5194/angeo-23-1747-2005, 2005.

Harrison, R., Nicoll, K., Ulanowski, Z., and Mather, T.: Self-charging of the Eyjafjallajökull volcanic ash plume, Environmental Research Letters, 5, doi:10.1088/1748-9326/5/2/024004, 2010.

Helling, C. and Woitke, P.: Dust in brown dwarfs - V. Growth and evaporation of dirty dust grains, Astronomy and Astrophysics, 455, 325–H4, doi:10.1051/0004-6361:20054598, 2006.

Helling, C., Dehn, M., Woitke, P., and Hauschildt, P.: Consistent simulations of substellar atmospheres and nonequilibrium dust cloud formation, Astrophysical Journal Letters, 675, 105–108, doi:10.1086/533462, 2008a.

Helling, C., Woitke, P., and Thi, W.: Dust in brown dwarfs and extra-solar planets - I. Chemical composition and spectral appearance of quasi-static cloud layers, Astronomy and Astrophysics, 485, 547–560, doi:10.1051/0004-6361:20078220, 2008b.

Helling, C., Jardine, M., and Mokler, F.: Ionization in atmospheres of brown dwarfs and extrasolar planets. I. Dust-induced collisional ionization, Astrophysical Journal, 737, doi:10.1088/0004-637X/737/1/38, 2011a.

Helling, C., Jardine, M., Witte, S., and Diver, D.: Ionization in atmospheres of brown dwarfs and extrasolar planets. I. The role of electron avalanche, Astrophysical Journal, 727, doi:10.1088/0004-637X/727/1/4, 2011b.

Helliwell, R.: Whistlers and related ionospheric phenomena, Stanford University Press, California, 1965.

Hess, W.: The artificial radiation belt made on July 9, 1962, Journal of Geophysical Research, 68, 667–683, doi:10.1029/JZ068i003p00667, 1963.

Hibbens, R., Freeman, M., Milan, S., and Ruohoniemi, J.: Winds and tides in the mid-latitude Southern hemisphere upper atmosphere recorded with the Falkland Islands SuperDARN radar, Annales Geophysicae, 29, 1985–1996, doi:10.5194/angeo-29-1985-2011, 2011.

Honary, F., Robinson, T., Wright, D., Stocker, A., Rietveld, M., and McCrea, I.: First direct observations of the reduced striations at pump frequencies close to the electron gyroharmonics, Annales Geophysicae, 17, 1235–1238, doi:10.1007/s005850050848, 1999.

Honary, F., Marple, S., Barratt, K., Chapman, P., Grill, M., and Nielsen, E.: Digital Beam-forming Imaging Riometer Systems, Review of Scientific Instruments, 82, 1–15, doi:10.1063/1.3567309, 2011.

Hosokawa, K., Ogawa, T., Arnold, N., Lester, M., Sato, N., and Yukimatu, A.: Extraction of polar mesosphere summer echoes from SuperDARN data, Geophysical Research Letters, 32, 1–4, doi:10.1029/2005GL022788, 2005.

Ignaccolo, M., Farges, T., Mika, A., Allin, T., Chanrion, O., Blanc, E., Neubert, T., Fraser-Smith, A., and Füllekrug, M.: The planetary rate of sprite events, Geophysical Research Letters, 33, 1–4, 2006.

Inan, U., Bell, T., Bortnik, J., and Albert, J.: Controlled precipitation of radiation belt electrons, Journal of Geophysical Research, 108, 1186, doi:10.1029/2002JA009580, 2003.

Inan, U., Piddyachiy, D., Peter, W., Sauvaud, J., and Parrot, M.: DEMETER satellite observations of lightning-induced electron precipitation, Geophysical Research Letters, 34, 1–5, doi:10.1029/2006GL029238, 2007.

Jarvis, M., Hibbins, R., Taylor, M., and Rosenberg, T.: Utilizing riometry to observe gravity waves in the sunlit mesosphere, Geophysical Research Letters, 30, 1–4, doi:10.1029/2003GL017885, 2003.

Kavanagh, A., Kosch, M., Honary, F., Senior, A., Marple, S., Woodfield, E., and McCrea, I.: The statistical dependence of auroral absorption on geomagnetic and solar wind parameters, Annales Geophysicae, 22, 877–887, doi:10.5194/angeo-22-877-2004, 2004.

Kosch, M., Rietveld, M., Hagfors, T., and Leyser, T.: High-latitude HF-induced airglow displaced equatorwards of the pump beam, Geophysical Research Letters, 27, 2817–2820, doi:10.1029/2000GL003754, 2000.

Kosch, M., Honary, F., del Pozo, C., Marple, S., and Hagfors, T.: High-resolution mapping of the characteristic energy of precipitating auroral particles, Journal of Geophysical Research, 106, 28 925–28 937, doi:10.1029/2001JA900107, 2001.

Kosch, M., Rietveld, M., Kavanagh, A., Davis, C., Yeoman, T., Honary, F., and Hagfors, T.: High-latitude pump-induced optical emissions for frequencies close to the third electron gyro-harmonic, Geophysical Research Letters, 29, 2112–2115, doi:10.1029/2002GL015744, 2002.

Kosch, M., Pedersen, T., Rietveld, M., Gustavsson, B., Grach, S., and Hagfors, T.: Artificial optical emissions in the high-latitude thermosphere induced by powerful radio waves: an observational review, Advances in Space Research, 40, 365–376, doi:10.1016/j.asr.2007.02.061, 2007a.

Kosch, M., Pedersen, T., Mishin, E., Oyama, S., Hughes, J., Senior, A., Watkins, B., and Bristow, B.: Coordinated optical and radar observations of ionospheric pumping for a frequency pass through the second electron gyroharmonic at HAARP, Journal of Geophysical Research, 112, doi:10.1029/2006JA012146, 2007b.

Kosch, M., Ogawa, Y., Rietveld, M., Nozawa, S., and Fujii, R.: An analysis of pump-induced artificial ionospheric ion upwelling at EISCAT, Journal of Geophysical Research, 115, doi:10.1029/2010JA015854, 2010.

Kosch, M., Yiu, I., Anderson, C., Tsuda, T., Ogawa, Y., Nozawa, S., Aruliah, A., Howells, V., Baddeley, L., McCrea, I., and Wild, J.: Mesoscale observations of Joule heating near an auroral arc and ion-neutral collision frequency in the polar cap E region, Journal of Geophysical Research, 116, doi:10.1029/2010JA016015, 2011.

Krehbiel, P., Riousset, J., Pasko, V., Thomas, R., Rison, W., Stanley, M., and Edens, H.: Upward electrical discharges from thunderstorms, Nature Geoscience, 1, 233–237, doi:10.1038/ngeo162, 2008.

Le Bihan, N. and Sangwine, S.: Quaternion principal component analysis of color images, IEEE International Conference on Image Processing, 1, 809–812, 2003.

Lefeuvre, F., Blanc, E., Pinçon, J., Roussel-Dupré, R., Lawrence, D., Sauvaud, J., Rauch, J., Feraudy, H., and Lagoutte, D.: TARANIS- A satellite project dedicated to the physics of TLEs and TGFs, Space Science Reviews, 137, 301–315, doi:10.1007/s11214-008-9414-4, 2008.

Lefeuvre, F., Marshall, R., Pinçon, J., Inan, U., Lagoutte, D., Parrot, M., and Berthelier, J.: On remote sensing of transient luminous events' parent lightning discharges by ELF/VLF wave measurements on board a satellite, Journal of Geophysical Research, 114, 1–13, doi:10.1029/2009JA014154, 2009.

Lehtinen, N., Bell, T., and Inan, U.: Monte Carlo simulation of runaway MeV electron breakdown with application to red sprites and terrestrial gamma ray flashes, Journal of Geophysical Research, 104, 24 699–24 712, doi:10.1029/1999JA900335, 1999.

Lester, M.: SuperDARN: A network approach to geospace science in the 21st century, Journal of Atmospheric and Solar-Terrestrial Physics, 70, 2309–2323, doi:10.1016/j.jastp.2008.08.003, 2008.

Li, C., Ebert, U., and Hundsdorfer, W.: Spatially hybrid computations for streamer discharges: II. Fully 3D simulations, Journal of Computational Physics, 231, 1020–1050, doi:10.1016/j.jcp.2011.07.023, 2012.

Liszka, L.: On the possible infrasound generation by sprites, Journal of Low Frequency Noise Vibration and Active Control, 23, 85–93, doi:10.1260/0263092042869838, 2004.

Liszka, L. and Hobara, Y.: Sprite-attributed infrasonic chirps - their detection, occurrence and properties between 1994 and 2004, Jour-

nal of Atmospheric and Solar-Terrestrial Physics, 68, 1179–1188, doi: 10.1016/j.jastp.2006.02.016, 2006.

Liu, N. and Pasko, V.: Effects of photoionization on propagation and branching of positive and negative streamers in sprites, Journal of Geophysical Research, 109, doi:10.1029/2003JA010064, 2004.

Lu, G., Cummer, S., Li, J., Han, F., Smith, D., and Grefenstette, B.: Characteristics of broadband lightning emissions associated with terrestrial gamma ray flashes, Journal of Geophysical Research, 116, 1–12, doi: 10.1029/2010JA016141, 2011.

Lyons, L., Thorne, R., and Kennel, C.: Pitch-angle diffusion of radiation belt electrons within the plasmasphere, Journal of Geophysical Research, 77, 3455, doi:10.1029/JA077i019p03455, 1972.

MacGorman, D. and Rust, W.: The electrical nature of storms, Oxford University Press, New York, 1998.

MacLachlan, C., Diver, D., and Potts, H.: The evolution of electron overdensities in magnetic fields, New Journal of Physics, 11, doi:10.1088/1367-2630/11/6/063001, 2009.

Mallat, S.: A wavelet tour of signal processing. The sparse way. Third edition. With contributions from Gabriel Peyré, Elsevier/Academic Press, Amsterdam, 2009.

Marshall, R.: An improved model of the lightning electromagnetic field interaction with the D-region ionosphere, Journal of Geophysical Research, 117, 1–15, doi:10.1029/2011JA017408, 2012.

Marshall, T., McCarthy, M., and Rust, W.: Electric field magnitudes and lightning initiation in thunderstorms, Journal of Geophysical Research, 100, 7097–7103, doi:10.1029/95JD00020, 1995.

Massines, F., Rabehi, A., Decomps, P., Ben Gadri, R., Ségur, P., and Mayoux, C.: Experimental and theoretical study of a glow discharge at atmospheric pressure controlled by dielectric barrier, Journal of Applied Physics, 83, 2950–2957, doi:10.1063/1.367051, 1998.

Mather, T. and Harrison, R.: Electrification of volcanic plumes, Surveys in Geophysics, 27, 387–432, doi:10.1007/s10712-006-9007-2, 2006.

McConville, S., Speirs, D., Ronald, K., Phelps, A., Cross, A., Bingham, R., Robertson, C., Whyte, C., He, W., Gillespie, K., Vorgul, I., Cairns, R., and Kellett, B.: Demonstration of auroral radio emission mechanisms by laboratory experiment, Plasma Physics and Controlled Fusion, 50, doi: 10.1088/0741-3335/50/7/074010, 2008.

Mende, S., Chang, Y., Chen, A., Frey, H., Fukunishi, H., Geller, S., Harris, S., Heetderks, H., Hsu, R., Lee, L., Su, H., and Takahashi, Y.: Spacecraft based studies of transient luminous Events, in: Sprites, Elves and Intense Lightning Discharges, edited by Füllekrug, M., Mareev, E., and Rycroft, M., vol. NATO Science Series II, 225, Springer, Dordrecht, The Netherlands, 2006.

Meredith, N., Horne, R., Glauert, S., Baker, D., Kanekal, S., and Albert, J.: Relativistic electron loss timescales in the slot region, Journal of Geophysical Research, 114, doi:10.1029/2008JA013889, 2009.

Milan, S., Davies, J., and Lester, M.: Coherent HF radar backscatter characteristics associated with auroral forms identified by incoherent radar techniques, Journal of Geophysical Research, 104, 22 591–22 603, doi: 10.1029/1999JA900277, 1999.

Miron, S., Le Bihan, N., and Mars, J.: Quaternion-MUSIC for vector-sensor array processing, IEEE Transactions on Signal Processing, 54, 1218–1229, doi:10.1109/TSP.2006.870630, 2006.

Moss, G., Pasko, V., Liu, N., and Veronis, G.: Monte Carlo model for analysis of thermal runaway electrons in streamer tips in transient luminous events and streamer zones of lightning leaders, Journal of Geophysical Research, 111, 1–37, doi:10.1029/2005JA011350, 2006.

Neubert, T., Rycroft, M., Farges, T., Blanc, E., Chanrion, O., Arnone, E., Odzimek, A., Arnold, N., Enell, C., Turunen, E., Bösinger, T., Mika, A., Haldoupis, C., Steiner, R., Van der Velde, O., Soula, S., Berg, P., Boberg, F., Thejll, P., Christiansen, B., Ignaccolo, M., Füllekrug, M., Verronen, P., Montanya, J., and Crosby, N.: Recent results from studies of electric discharges in the mesosphere, Surveys in Geophysics, 29, 71–137, doi:10.1007/s10712-008-9043-1, 2008.

Nguyen, C., van Deursen, A., van Heesch, E., Winands, G., and Pemen, J. M.: X-ray emission in streamer-corona plasma, Journal of Physics D: Applied Physics, 43, doi:10.1088/0022-3727/43/2/025202, 2010.

Nicoll, K., Harrison, R., and Ulanowski, Z.: Observations of Saharan dust layer electrification, Enrionmental Research Letters, 6, doi:10.1088/1748-9326/6/1/014001, 2011.

Nijdam, S., van der Wetering, F., Blanc, R., van Veldhuizen, E., and Ebert, U.: Probing photo-ionization: experiments on positive streamers in pure gases and mixtures, Journal of Physics D: Applied Physics, 43, doi:10.1088/0022-3727/43/14/145204, 2010.

Odzimek, A., Kubicki, M., Lester, M., and Grocott, A.: Relation between the SuperDARN ionospheric potential and ground electric field at polar station Hornsund, Proceedings of the 14th International Conference on Atmospheric Electricity - ICAE, 115, 1–22, doi:10.1029/2009JD013341, 2011.

Ogawa, T., Arnold, N., Kirkwood, S., Nishitani, N., and Lester, M.: Finland HF and Esrange MST radar observations of polar mesosphere summer echoes, Annales Geophysicae, 21, 1047–1055, doi:10.5194/angeo-21-1047-2003, 2003.

Østgaard, N., Gjesteland, T., Hanson, R., Collier, A., and Carlson, B.: The true fluence distribution of terrestrial gamma ray flashes at satellite altitudes, Journal of Geophysical Research, 117, 1–8, doi:10.1029/2011JA017365, 2012.

Pai, D., Lacoste, D., and Laux, C.: Transitions between corona, glow, and spark regimes of nanosecond repetitively pulsed discharges in air at atmospheric pressure, Journal of Physics D: Applied Physics, 107, 1–15, doi: 10.1063/1.3309758, 2010.

Parrot, M., Inan, U., Lehtinen, N., and Pincon, J.: Penetration of lightning MF signals to the upper ionosphere over VLF ground-based transmitters,

Journal of Geophysical Research, 114, doi:10.1029/2009JA014598, 2009.
Pasko, V.: Red sprite discharges in the atmosphere at high altitude: the molecular physics and the similarity with laboratory discharges, Plasma Sources Science and Technology, 16, 13–29, doi:10.1088/0963-0252/16/1/S02, 2007.
Pasko, V.: Recent advances in theory of transient luminous events, Journal of Geophysical Research, 115, 1–24, doi:10.1029/2009JA014860, 2010.
Pasko, V. and Snively, J.: Mechanism of infrasound radiation from sprites, EOS Transactions of AGU, Fall Meeting Abstract AE23A0899, 88, 2007.
Pasko, V., Stanley, M., Mathews, J., Inan, U., and Wood, T.: Electrical discharge from a thundercloud top to the lower ionosphere, Nature, 416, 152–154, doi:10.1038/416152a, 2002.
Rakov, V. and Uman, M.: Lightning, Physics and Effects, Cambridge University Press, Cambridge, 2003.
Randall, C., Siskind, D., and Bevilacqua, R. M.: Stratospheric NOx enhancements in the Southern Hemisphere vortex in winter/spring of 2000, Geophysical Research Letters, 28, 2385–2388, doi:10.1029/2000GL012746, 2001.
Reising, S., Inan, U., Bell, T., and Lyons, W.: Evidence for continuing currents in sprite-producing lightning flashes, Geophysical Research Letters, 23, 3639–3642, doi:10.1029/96GL03480, 1996.
Renard, J., Brogniez, C., Berthet, G., Bourgeois, Q., Gaubicher, B., Chartier, M., Balois, J., Verwaerde, C., Auriol, F., Francois, P., Daugeron, D., and Engrand, C.: Vertical distribution of the different types of aerosols in the stratosphere, Journal of Geophysical Research, 113, doi:10.1029/2008JD010150, 2008.
Renard, J., Berthet, G., Salazar, V., Catoire, V., Tagger, M., Gaubicher, B., and Claude, R.: In situ detection of aerosol layers in the middle stratosphere, Geophysical Research Letters, 37, doi:10.1029/2010GL044307, 2010.
Riousset, J., Pasko, V., and Bourdon, A.: Air-density-dependent model for analysis of air heating associated with streamers, leaders, and transient luminous events, Journal of Geophysical Research, 115, 1–22, doi:10.1029/2010JA015918, 2010.
Rishbeth, H. and van Eyken, A.: EISCAT: early history and the first ten years of operation, Journal of Atmospheric and Terrestrial Physics, 55, 525–542, doi:10.1016/0021-9169(93)90002-G, 1993.
Robinson, T., Honary, F., Stocker, A., Jones, T., and Stubbe, P.: First EISCAT observations of the modification of F-region electron temperature during heating at harmonics of the electron gyrofrequency, Journal of Atmospheric and Terrestrial Physics, 58, 385–395, doi:10.1016/0021-9169(95)00043-7, 1996.
Roble, R.: On modeling component processes in the Earth's global electric circuit, Journal of Atmospheric and Terrestrial Physics, 53, 831–847, doi:10.1016/0021-9169(91)90097-Q, 1991.
Ronald, K., Speirs, D., McConville, S., Gillespie, K., Phelps, A., Bingham, R., Vorgul, I., Cairns, R., Cross, A., Robertson, C., Whyte, C., He, W., and Kellett, B.: Auroral magnetospheric cyclotron emission processes: numerical and experimental simulations, Plasma Physics and Controlled Fusion, 53,

doi:10.1088/0741-3335/53/7/074015, 2011.

Roussel-Dupré, R. and Gurevich, A.: On runaway breakdown and upward propagating discharges, Journal of Geophysical Research, 101, 2297–2311, doi:10.1029/95JA03278, 1996.

Roussel-Dupré, R., Symbalisty, E., Taranenko, Y., and Yukhimuk, V.: Simulations of high-altitude discharges initiated by runaway breakdown, Journal of Atmospheric and Solar-Terrestrial Physics, 60, 917–940, doi:10.1016/S1364-6826(98)00028-5, 1998.

Ruohoniemi, J. and Baker, K.: Large-scale imaging of high-latitude convection with Super Dual Auroral Radar Network HF radar observations, Journal of Geophysical Research, 103, 20 797–20 811, doi:10.1029/98JA01288, 1998.

Rycroft, M. and Harrison, R.: Electromagnetic atmosphere-plasma coupling: The global atmospheric electric circuit, Space Science Reviews, published online, doi:10.1007/s11214-011-9830-8, 2011.

Rycroft, M. and Odzimek, A.: Effects of lightning and sprites on the ionospheric potential, and threshold effects on sprite initiation, obtained using an analog model of the global atmospheric electric circuit, Journal of Geophysical Research, 115, 1–18, doi:10.1029/2009JA014758, 2010.

Rycroft, M., Odzimek, A., Arnold, N., Fullekrug, M., Kulak, A., and Neubert, T.: New model simulations of the global atmospheric electric circuit driven by thunderstorms and electrified shower clouds: The roles of lightning and sprites, Journal of Atmospheric and Solar-Terrestrial Physics, 69, 2485–2509, doi:10.1016/j.jastp.2007.09.004, 2007.

Rycroft, M., Harrison, R., Nicoll, K., and Mareev, E.: An overview of Earth's global electric circuit and atmospheric conductivity, Space Science Reviews, 137, 83–105, doi:10.1007/s11214-008-9368-6, 2008.

Rycroft, M., Nicoll, K., Aplin, K., and Harrison, R.: Recent advances in global electric circuit coupling between the space environment and the troposphere, Journal of Atmospheric and Solar-Terrestrial Physics, published online, doi:10.1016/j.jastp.2012.03.015, 2012.

Saunders, C. and Rimmer, J.: The electric field alignment of ice crystals in thunderstorms, Atmospheric Research, 51, 337–343, doi:10.1016/S0169-8095(99)00018-6, 1999.

Sauvaud, J., Moreau, T., Maggiolo, R., Treilhou, J., Jacquey, C., Cros, A., Coutelier, J., Rouzaud, J., Penou, E., and Gangloff, M.: High-energy electron detection onboard DEMETER: The IDP spectrometer, description and first results on the inner belt, Planetary and Space Science, 54, 502–511, doi:10.1016/j.pss.2005.10.019, 2006.

Sauvaud, J., Maggiolo, R., Jacquey, C., Parrot, M., Berthelier, J., Gamble, R., and Rodger, C.: Radiation beltt electron precipitation due to VLF transmitters: Satellite observations, Geophysical Research Letters, 35, 1–5, doi:10.1029/2008GL033194, 2008.

Sauvaud, J., Walt, M., Delcourt, D., Benoist, C., Penou, E., Chen, Y., and Russell, C.: Inner radiation belt particle acceleration and energy structuring by drift resonance with ULF waves during storms, submitted to J. Geophys. Res., 2012.

Schisselé, E., Guilbert, J., Gaffet, S., and Cansi, Y.: Accurate time-frequency-wave number analysis to study coda waves, Geophysical Journal International, 158, 577–591, doi:10.1111/j.1365-246X.2004.02211.x, 2004.

Schisselé, E., Gaffet, S., and Cansi, Y.: Characterization of regional and local scattering effects from small-aperture seismic array recordings, Journal of Seismology, 9, 137–149, doi:10.1007/s10950-005-8234-1, 2005.

Sentman, D. and Wescott, E.: Observations of upper atmospheric optical flashes recorded from an aircraft, Geophysical Research Letters, 20, 2857–2860, doi:10.1029/93GL02998, 1993.

Sentman, D., Wescott, E., Osborne, D., Hampton, D., and Heavner, M.: Preliminary results from the Sprites94 aircraft campaign: 1. Red sprites, Geophysical Research Letters, 22, 1205–1208, doi:10.1029/95GL00583, 1995.

Sentman, D., Wescott, E., Picard, R., Winick, J., Stenbaek-Nielsen, H., Dewan, E., Moudry, D., Sabbas, F. S., Heavner, M., and Morrill, J.: Simultaneous observations of mesospheric gravity waves and sprites generated by a midwestern thunderstorm, Journal of Atmospheric and Solar-Terrestrial Physics, 65, 537–500, doi:10.1016/S1364-6826(02)00328-0, 2003.

Seppälä, A., Verronen, P., Clilverd, M., C.E.Randall, Tamminen, J., Sofieva, V., Backman, L., and Kyrola, E.: Arctic and Antarctic polar winter NOx and energetic particle precipitation in 2002-2006, Geophysical Research Letters, 34, doi:10.1029/2007GL029733, 2007.

Seppälä, A., Randall, C., Clilverd, M., Rozanov, E., Harvey, V., and Rodger, C.: Geomagnetic activity and polar surface air temperature variability, Journal of Geophysical Research, 114, doi:10.1029/2008JA014029, 2009.

Shao, X., Hamlin, T., and Smith, D.: A closer examination of terrestrial gamma-ray flash-related lightning processes, Journal of Geophysical Research, 115, 1–8, doi:10.1029/2009JA014835, 2010.

Siingh, D., Singh, A., Patel, R., Singh, R., Singh, R., Veenadhari, B., and Mukherjee, M.: Thunderstorms, lightning, sprites and magnetospheric whistler-mode radio waves, Surveys in Geophysics, 29, 499–551, doi:10.1007/s10712-008-9053-z, 2008.

Siingh, D., Singh, R., Singh, A., Kumar, S., Kulkarni, M., and Singh, K.: Discharges in the stratosphere and mesosphere, Space Science Reviews, 169, 1–49, doi:10.1007/s11214-012-9906-0, 2012.

Slevin, P. and Harrison, W.: Hollow-cathode discharge as a spectrochemical emission source, Applied Spectroscopy Reviews, 10, 201–255, doi:10.1080/05704927508085065, 1975.

Smith, D., Lopez, L., Lin, R., and Barrington-Leigh, C.: Terrestrial gamma-ray flashes observed up to 20 MeV, Science, 307, 1085–1088, doi:10.1126/science.1107466, 2005.

Soula, S., Van der Velde, O., Montanyà, J., Neubert, T., Chanrion, O., and Ganot, M.: Analysis of thunderstorm and lightning activity associated with sprites observed during the EuroSprite campaigns: Two case studies, Atmospheric Research, 91, 514–528, doi:10.1016/j.atmosres.2008.06.017, 2009.

Soula, S., Van der Velde, O., Palmieri, J., Chanrion, O., Neubert, T., Montanya, J., Gangneron, F., Meyerfeld, Y., Lefeuvre, F., and Lointier, G.:

Characteristics and conditions of production of transient luminous events observed over a maritime storm, Journal of Geophysical Research, 115, doi: 10.1029/2009JD012066, 2010.

Soula, S., Van der Velde, O., Montanya, J., Huet, P., Barthe, C., and Bor, J.: Characteristics and conditions of production of transient luminous events observed over a maritime storm, Journal of Geophysical Research, 116, doi: 10.1029/2010JD015581, 2011.

Speirs, D., McConville, S., Gillespie, K., Ronald, K., Phelps, A., Cross, A., Bingham, R., Robertson, C., Whyte, C., Vorgul, I., Cairns, R., and Kellett, B.: Numerical simulation of auroral cyclotron maser processes, Plasma Physics and Controlled Fusion, 50, doi:10.1088/0741-3335/50/7/074011, 2008.

Stanley, M., Shao, X., Smith, D., Lopez, L., Pongratz, M., Harlin, J., Stock, M., and Regan, A.: A link between terrestrial gamma-ray flashes and intracloud lightning discharges, Geophysical Research Letters, 33, 1–4, doi: 10.1029/2005GL025537, 2006.

Stark, C., Diver, D., da Costa, D., and Laing, E.: Nonlinear mode coupling in pair plasmas, Astronomy and Astrophysics, 476, 17–30, doi:10.1051/0004-6361:20077988, 2007.

Starks, M., Quinn, R., Ginet, G., Albert, J., Sales, G., Reinisch, B., and Song, P.: Illumination of the plasmasphere by terrestrial very low frequency transmitters: Model validation, Journal of Geophysical Research, 113, 1–16, 2008.

Starks, M., Bell, T., Quinn, R., Inan, U., Piddyachiy, D., and Parrot, M.: Modeling of Doppler-shifted terrestrial VLF transmitter signals observed by DEMETER, Geophysical Research Letters, 36, 1–6, doi: 10.1029/2009GL038511, 2009.

Stubbe, P.: Review of ionospheric modification experiments at Tromso, Journal of Atmospheric and Terrestrial Physics, 58, 349–368, doi:10.1016/0021-9169(95)00041-0, 1996.

Su, H., Su, R., Chen, A., Wang, Y., Hsiao, W., Lai, W., Lee, L., Sato, M., and Fukunishi, H.: Gigantic jets between a thundercloud and the ionosphere, Nature, 423, 974–976, doi:10.1038/nature01759, 2003.

Tavani, M., Marisaldi, M., Labanti, C., and et al.: Terrestrial gamma-ray flashes as powerful particle accelerators, Physical Review Letters, 106, 1–5, doi:10.1103/PhysRevLett.106.018501, 2011.

Thorne, R. and Horne, R.: Landau damping of magnetospherically reflected whistlers, Journal of Geophysical Research, 99, 17,249–17,258, doi: 10.1029/94JA01006, 1994.

Thorne, R., O'Brien, T., Shprits, Y., Summers, D., and Horne, R.: Timescale for MeV electron microburst loss during geomagnetic storms, Journal of Geophysical Research, 110, doi:10.1029/2004JA010882, 2005.

Townsend, J.: The conductivity produced in gases by the motion of negatively charged ions, Philosophical Magazine Series, 6, 198–227, doi: 10.1080/14786440109462605, 1901.

Trakhtengerts, V. and Rycroft, M.: Whistler and Alfvén mode cyclotron masers in space, Cambridge atmospheric and space science series, Cam-

bridge University Press, 2008.
Tripathi, S., Vishnoi, S., Kumar, S., and Harrison, R.: Computationally efficient expressions for the collision efficiency between electrically charged aerosol particles and cloud droplets, Quarterly Journal of the Royal Meteorological Society, 132, 1717–1731, doi:10.1256/qj.05.125, 2006.
Ulanowski, Z., Bailey, J., Lucas, P., Hough, J., and Hirst, E.: Alignment of atmospheric mineral dust due to electric field, Atmospheric Chemistry and Physics, 7, 6161–6173, doi:10.5194/acp-7-6161-2007, 2007.
Van der Velde, O., Mika, A., Soula, S., Haldoupis, C., Neubert, T., and Inan, U.: Observations of the relationship between sprite morphology and in-cloud lightning processes, Journal of Geophysical Research, 111, doi:10.1029/2005JD006879, 2006.
Van der Velde, O., Montanyá, J., Soula, S., Pineda, N., and Bech, J.: Spatial and temporal evolution of horizontally extensive lightning discharges associated with sprite-producing positive cloud-to-ground flashes in northeastern Spain, Journal of Geophysical Research, 115, 1–17, doi:10.1029/2009JA014773, 2010.
Van Veldhuizen, E.: Electrical discharges for environmental purposes: fundamentals and applications, Nova Science, New York, 2000.
Vernier, J., Pommereau, J., Garnier, A., Pelon, J., Larsen, N., Nielsen, J., Christensen, T., Cairo, F., Thomason, L., Leblanc, T., and McDermid, I.: Tropical stratospheric aerosol layer from CALIPSO lidar observations, Journal of Geophysical Research, 114, doi:10.1029/2009JD011946, 2009.
Wait, J. and Spies, K.: Characteristics of the Earth-ionosphere wave guide for VLF radio waves, Technical Note 300, National Bureau of Standards, 1964.
Walt, M.: Effects of atmospheric collisions on geomagnetically trapped electrons, Journal of Geophysical Research, 69, 3947–3958, doi:10.1029/JZ069i019p03947, 1964.
Wescott, E., Sentman, D., Osborne, D., Hampton, D., and Heavner, M.: Preliminary results from the Sprites94 aircraft campaign: 2. Blue jets, Geophysical Research Letters, 22, 1209–1212, doi:10.1029/95GL00582, 1995.
Wilson, C.: On some determinations of the sign and magnitude of electric discharges in lightning flashes, Proc. Roy. Soc. London, 92, 555–574, doi:10.1098/rspa.1916.0040, 1916.
Wilson, C.: Investigations on lightning discharges and on the electric field of thunderstorms, Philosophical Transactions of the Royal Society of London A, 221, 73–115, doi:10.1098/rsta.1921.0003, 1921.
Wilson, C.: The electric field of a thundercloud and some of its effects, Proceeding of the Physical Society, London, 37, 32D–37D, doi:10.1088/1478-7814/37/1/314, 1924.
Wilson, C.: Some thundercloud problems, J. Franklin Inst., 208, 1–12, doi:10.1016/S0016-0032(29)90935-2, 1929.
Witte, S., Helling, C., and P.H. Hauschildt, P. H.: Dust in brown dwarfs and extra-solar planets II. Cloud formation for cosmologically evolving abundances, Astronomy and Astrophysics, 506, 1367–1380, doi:10.1051/0004-6361/200811501, 2009.

Woitke, P. and Helling, C.: Dust in brown dwarfs - II. The coupled problem of dust formation and sedimentation, Astronomy and Astrophysics, 399, 297–313, doi:10.1051/0004-6361:20021734, 2003.

Xu, W., Celestin, S., and Pasko, V.: Source altitudes of terrestrial gamma-ray flashes produced by lightning leaders, Journal of Geophysical Research, 39, 1–5, doi:10.1029/2012GL051351, 2012.

Yair, Y., Israelevich, P., Devir, A., Price, C., Joseph, J., Levin, Z., Ziv, B., Sternlieb, A., and Teller, A.: New observations of sprites from the space shuttle, Journal of Geophysical Research, 109, 1–10, doi:10.1029/2003JD004497, 2004.

Yalandin, M., Shpak, V., Shunailov, S., Oulmaskoulov, M., Ginzburg, N., Zotova, I., Novozhilova, Y., Sergeev, A., Phelps, A., Cross, A., Wiggins, S., and Ronald, K.: Generation of powerful subnanosecond microwave pulses in the range of 38-150 GHz, IEEE Transactions on Plasma Science, 28, 1615–1619, doi:10.1109/27.901243, 2000.